

Oil & Natural Gas Technology

DOE Award No.: DE-FE0024297

Quarterly Research Performance Progress Report

(Period ending: 09/30/2017)

Marcellus Shale Energy and Environment Laboratory (MSEEL)

Project Period: October 1, 2014 – September 30, 2019

Submitted by:
Samuel Taylor



West Virginia University Research Corporation
DUN's Number: 191510239
886 Chestnut Ridge Road,
PO Box 6845, Morgantown WV, 26505
Tim.Carr@mail.wvu.edu
304-293-9660

Prepared for:
United States Department of Energy
National Energy Technology Laboratory

October 31, 2017



Office of Fossil Energy

Quarterly Progress Report

July 1 – September 30, 2017

Executive Summary

The objective of the Marcellus Shale Energy and Environment Laboratory (MSEEL) is to provide a long-term field site to develop and validate new knowledge and technology to improve recovery efficiency and minimize environmental implications of unconventional resource development.

This quarter was focused on the rollout of additional technical analysis work in several areas pursuant to a DOE scope increase in August. The team has started to develop concepts for future data collection or sampling efforts from new wells, to be decided on at the end of CY17. An External Advisory Committee meeting is scheduled for October 10, 2017 in Morgantown, WV, to discuss project technical results to date, to address any data gaps in the current suite of research findings, and to propose concepts for future work. Finally, the program was selected for a DOE Peer Review. The team had significant effort in collecting and collating data, publications, and other deliverables as part of this effort. The Peer Review Meeting is currently scheduled for early December 2017.

Deliverables this quarter include:

Papers from the Summer 2017 URTeC session area available. They are not included with this report due to size, but can be downloaded from the MSEEL portal (<http://www.mseel.org/research/>).

The project team is tracking nine (9) milestones in this budget period:

3/1/2017 - Completed Production Logging (Scheduled 2/15/2017; Completed 3/15/2017)

4/30/17 - Conduct preliminary analysis of production log data and present to DOE. (Completed and being worked into a new reservoir simulation – Review meeting held at WVU 4/11/2017)

6/30/2017 - Initial economic impact assessment completed (Scheduled 6/30/2017; Completed 6/30/2017)

8/15/17 - Coordinate and hold MSEEL session at URTEC 2017 (Scheduled 8/30/2017; Completed 8/30/2017)

8/30/17 - Complete rock geochemistry and geomechanical data analysis and integration with log & microseismic data to develop preliminary reservoir simulation and fracture model(s) Simulation model is providing a good history match. (Scheduled 8/30/2017; Completed 8/30/2017)

8/30/17 – Create a comprehensive online library of MSEEL presentations and papers that can be downloaded. Maintain with additional material through end of project. (Scheduled 8/30/2017; Completed 9/30/2017)

8/30/17 – Reorganize MSEEL data portal and prepare to transfer to NETL for public dissemination. Data will be made public in December after the 2 year time period. (Original Schedule 8/30/2017; Revised plan for 12/30/2017)

12/31/17 – Complete a detailed reservoir simulation incorporating fracture geometry and flow simulation

12/31/17 - Determine changes in kerogen structure and bulk rock interactions and composition on interaction with fracturing fluids under simulated subsurface conditions.

Quarterly Progress Report

July 1 – September 30, 2017

Project Performance

This report summarizes the activities of Cooperative Agreement DE-FE0024297 (Marcellus Shale Energy and Environment Laboratory – MSEEL) with the West Virginia University Research Corporation (WVURC) during the fourth quarter of FY2017 (July 1 through September 30, 2017).

This report outlines the approach taken, including specific actions by subtopic. If there was no identified activity during the reporting period, the appropriate section is included but without additional information.

A summary of major lessons learned to this point of the project are provided as bullet points and will be added to as research is completed. New lessons are **highlighted**.

- 1) Synthetic based drilling mud is ecofriendly as well as helps with friction which resulted in faster drilling and reduced costs while leading to drilling waste from both the vertical and horizontal portions of the wells that passed all toxicity standards.
- 2) Microseismic monitoring does not completely define propped fractures and the extent of stimulated reservoir volume from hydraulic fracture stimulation. Requires integration of data from core, logs and slow slip seismic monitoring.
- 3) Production logging documents significant variations in production between completion types, stages and even clusters. Variations in production provide the necessary data for robust reservoir simulation.
- 4) Complex geology in laterals can lead to intercommunication between stages and reduced fracture stimulation efficiency. This can be mitigated with limited entry (engineered completions) that significantly improves fracture stimulation efficiency. NNE has continued the practice in subsequent wells. Planned production logging will help to define production efficiency.
- 5) The significant part of air emissions are in truck traffic, not in drilling and fracture operations on the pad. Emissions from both the pad and trucking can be reduced with operational modifications such as reducing dust and truck traffic during fracture stimulation (e.g., Sandbox) from bifuel (natural gas-diesel) engine operations.
- 6) Dual fuel engines demonstrated lower carbon monoxide (CO) emissions than diesel only operation. Dual fuel operations could reduce onsite diesel fuel consumption by 19 to 63% for drilling and 52% for hydraulic stimulation.
- 7) Biologic activity cannot be eliminated with biocides, only delayed. The biologic activity results in a unique biota that may affect operations. There may be other methods to control/influence biologic activity.
- 8) Water production changes rapidly after fracture stimulation in terms of volume (500 bbl/day to less than 1 bbl/day) and total dissolved solids (TDS from freshwater, 100 to 150g/L). Radioactivity is associated with produced water, not drill cuttings.
- 9) Drill cutting radioactivity levels were within West Virginia DEP standards of 5 pCi/g above background. This was true of both vertical and horizontal (Marcellus) sections.
- 10) Using the green drilling fluid Bio-Base 365, all drill cutting samples, vertical and horizontal, passed the USEPA's method 1311 (Toxicity Characteristics Leaching Procedure or TCLP) for inorganic and organic contaminants. This indicates that under Federal and West Virginia solid waste rules, these solid wastes would not be considered hazardous.

- 11) The absence of hazardous TCLP findings suggest that drilling fluids, not the inherent properties of the Marcellus formation, play the dominant role in determining drill cutting toxicity.
- 12) Concerning produced water quality, hydraulic fracturing fluid was nearly identical to makeup (Monongahela River) water. Initial produced water underwent a radical change in ionic composition and a two order of magnitude increase in total dissolved solids (TDS).
- 13) Produced water is highly saline and total dissolved solids (TDS) rapidly increased to a maximum between 100 and 150 g/L. There was negligible change in ionic composition between the initially produced water and that sampled five years post completion.
- 14) Concentrations of both 226 Ra and 228 Ra increased rapidly through the produced water cycle to combined maximum concentrations of 20,000 pCi/L in the first year post completion. These radium isotopes are critical regulatory determinants.
- 15) The volume of produced water decreased rapidly from nearly 500 bbl/day to less than 1 bbl/day after one year. Over this cycle produced water averaged about 6 bbl/day.
- 16) Developed a new frequency attribute calculated from the DAS data that reveals cross-stage fluid communication during hydraulic fracturing.

Initial results presented at the ESAAPG Meeting in Morgantown, WV on 27 September and manuscript is being prepared for Society of Petroleum Engineers Hydraulic Fracturing Conference.

Project Management Update

Approach

The project management team will work to generate timely and accurate reporting, and to maintain project operations, including contracting, reporting, meeting organization, and general oversight.

Results and Discussion

This quarter was focused on the rollout of additional technical analysis work in several areas pursuant to a DOE scope increase in August. The team has started to develop concepts for future data collection or sampling efforts from new wells, to be decided on at the end of CY17. An External Advisory Committee meeting is scheduled for October 10, 2017 in Morgantown, WV, to discuss project technical results to date, to address any data gaps in the current suite of research findings, and to propose concepts for future work. Finally, the program was selected for a DOE Peer Review. The team had significant effort in collecting and collating data, publications, and other deliverables as part of this effort. The Peer Review Meeting is currently scheduled for early December 2017.

The project team is tracking nine (9) milestones in this budget period:

3/1/2017 - Completed Production Logging (Scheduled 2/15/2017; Completed 3/15/2017)

4/30/17 - Conduct preliminary analysis of production log data and present to DOE. (Completed and being worked into a new reservoir simulation – Review meeting held at WVU 4/11/2017)

6/30/2017 - Initial economic impact assessment completed (Scheduled 6/30/2017; Completed 6/30/2017)

8/15/17 - Coordinate and hold MSEEL session at URTEC 2017 (Scheduled 8/30/2017; Completed 8/30/2017)

8/30/17 - Complete rock geochemistry and geomechanical data analysis and integration with log & microseismic data to develop preliminary reservoir simulation and fracture model(s) Simulation model is providing a good history match. (Scheduled 8/30/2017; Completed 8/30/2017)

8/30/17 – Create a comprehensive online library of MSEEL presentations and papers that can be downloaded. Maintain with additional material through end of project. (Scheduled 8/30/2017; Completed 9/30/2017)

8/30/17 – Reorganize MSEEL data portal and prepare to transfer to NETL for public dissemination. Data will be made public in December after the 2 year time period. (Original Schedule 8/30/2017; Revised plan for 12/30/2017)

12/31/17 – Complete a detailed reservoir simulation incorporating fracture geometry and flow simulation

12/31/17 - Determine changes in kerogen structure and bulk rock interactions and composition on interaction with fracturing fluids under simulated subsurface conditions.

Production data for gas and water from the MSEEL 3H and 5H wells are presented through the end of the quarter (Figures 0.1). The fluctuating volumes from February through present is due to work-overs on the MIP-3H and curtailment of the other MIP 5H associated with production logging of the MIP-3H.

Water Production for MIP-3H, MIP-4H, MIP-5H, and MIP-6H

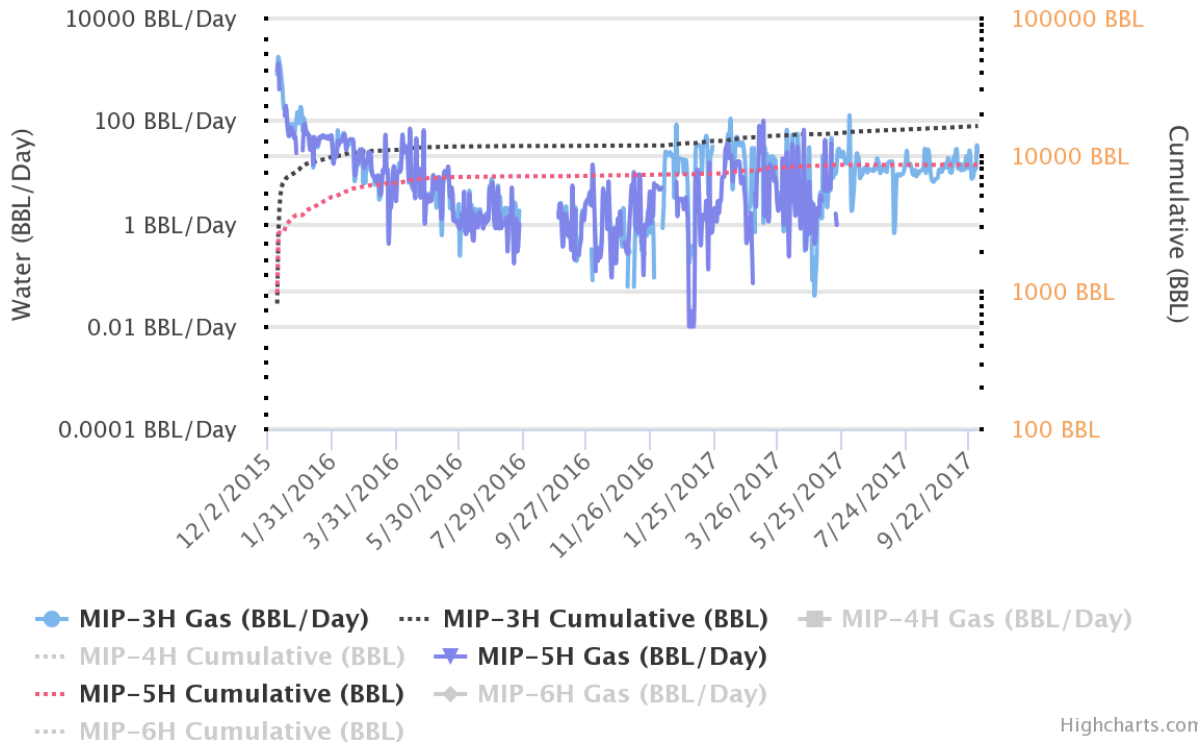


Figure 0.1 – Water production for the MIP-3H and MIP-5H showing the erratic data from February through present is due to work-overs on the MIP-3H and curtailment of the other MIP 5H associated with production logging of the MIP-3H.

Topic 1 – Geologic Engineering

Approach

This quarter, the research team continued core plug experiments. The permeability of the samples 59, 75, 78, 80, 84, 99, 102, 103, and 110 have been measured. Detailed analysis has been performed on Sample 80 and 103. The experiments on samples 101 and 101.2 have not been performed due to non-cylindrical shape of the plugs. Experiments on a new core plug have been initiated.

Results and Discussion

To determine absolute permeability, the modified Klinkenberg correction is necessary when the flow regime is transition flow, while Klinkenberg correction is sufficient under the slip flow conditions.

Measurement results indicated that the flow regime is transition flow for pore pressures below 900 psia, and it is slip flow for pore pressure above 1000 psia.

Work on the estimation of formation stress properties from drilling data has been completed.

Products

Elsaig, M., Black, S., Aminian, K., and S. Ameri, S.: "Measurement of Marcellus Shale Properties," SPE-87523, SPE Eastern Regional Conf., Lexington, KY, October 2017.

El Sgher, M., Aminian, K., and S. Ameri: "The Impact of Stress on Propped Fracture Conductivity and Gas Recovery in Marcellus Shale," SPE-189899, SPE Hydraulic Fracturing Technology Conf., Woodlands, TX, January 2018.

Ebusurra, M.: "Using Artificial Neural Networks to Predict Formation Stresses for Marcellus Shale with Data from Drilling Operations." MS Thesis, Petroleum & Natural Gas Engineering, West Virginia University, August 2017.

Plan for Next Quarter

The team will continue with core plug experiments, and analysis of the production and stimulation data to determine optimum well spacing and production decline performance.

Topic 2 – Geophysical & Geomechanical

Approach

Geophysical

The effort this past quarter concentrated on 1) putting together a presentation for the Annual SEG conference in Houston and making that presentation; 2) compilation of milestones/deliverables and accomplishments during the project.

Geomechanical

During this quarterly period, the influence of a discrete fracture network on the growth of hydraulic fractures was investigated through the use of numerical modeling. The model updated in the previous quarter was used to compute fracture dimensions for stage 11 through stage 20 of well MIP 3H.

Results & Discussion

Geophysical

As a follow up on the paper titled *Marcellus Shale model stimulation tests and microseismic response yield insights into mechanical properties and the reservoir DFN*: the paper was accepted with moderate revisions. Those revisions were completed last quarter and submitted. The team is still waiting on associate editor response.

Highlights of MSEEL geophysics and geomechanics studies from the G&G side

Wilson's early efforts were dedicated to several meetings with MSEEL team members, Northeast Natural Energy, and Schlumberger. Basic data were not collected until the Fall 2015. Initial data analysis and integration occupied the remainder of 2015 and has been ongoing since.

His presentation to NETL in August 2015 outlined several ideas associated with microseismic acquisition and analysis, reservoir fracture systems and their stimulation and basic geomechanics considerations.

The main outgrowths of initial data compilation and analysis were presented in Wilson, *et al.* (deliverable 9 below) at the Society of Exploration Geophysicists International Exposition and 86th Annual Meeting, Dallas, TX, October, 2016. A partial list of the deliverables leading up to this initial paper include:

- 1) Analysis of historical data related to natural and induced fracturing the Marcellus Shale conducted as part of the earlier Eastern Gas Shales program
- 2) Building a Petrel database that included vertical pilot well, the two horizontal wells (MIP-3H and MIP-5H) and all available logs from these wells
- 3) Building the microseismic data base from scratch and integrating it into the Petrel project.
- 4) Developing a structural interpretation of area based on stratigraphic penetrations observed in the horizontal and vertical wells
- 5) Building a geomechanical model with all cells populated by elastic parameters such as Young's modulus, Poisson's ratio, S_{min} , S_{max} (determined from stress anisotropy), etc.
- 6) Comprehensive analysis of all fracture image data leading to development of reservoir DFN and identification of the orientation of S_{Hmax} .
- 7) Multiple stimulation tests on the geomechanical model using actual hydraulic fracture treatment parameters and multiple DFN realizations
- 8) Iterative modifications to the model to obtain agreement between distribution of microseismic activity and stimulated DFN
- 9) Outgrowths compiled and presented in:

Thomas H. Wilson and Tim Carr, West Virginia University; B. J. Carney, Jay Hewitt, Ian Costello, Emily Jordon, Northeast Natural Energy LLC; Keith MacPhail, Oluwaseun Magbagbeola, Adrian Morales, Asbjorn Johansen, Leah Hogarth, Olatunbosun Anifowoshe, Kashif Naseem, Natalie Uschner, Mandy Thomas, Si Akin, Schlumberger, 2016, *Microseismic and model stimulation of natural fracture networks in the Marcellus Shale, West Virginia*: SEG International Exposition and 86th Annual Meeting, 3088-3092, <https://doi.org/10.1190/segam2016-13866107.1>.

In 2016 and 2017, another extensive study of elastic properties and their relationships to the presence of total organic carbon (TOC) was completed. The results of this study were presented in an additional paper (Wilson, *et al.*, deliverable 12 below). A partial list of deliverable items related to additional work include:

- 10) Calculate and analyze interrelationships between Lamé's parameters, various brittleness measures including those of Wang and Gale, Jarvie et al., and Greiser and Bray, $\lambda\rho$ and $\mu\rho$, and log derived elastic parameters.
- 11) Analyze all variables for possible relationship to TOC
- 12) Compile outgrowths into paper and present

Thomas H. Wilson*, Payam Kavousi, Tim Carr, West Virginia University; B. J. Carney, Northeast Natural Energy LLC; Natalie Uschner, Oluwaseun Magbagbeola and Lili Xu, Schlumberger, 2017, *Relationships of $\lambda\rho$ and $\mu\rho$, brittleness index, Young's modulus, Poisson's ratio and high TOC for the Marcellus Shale, Morgantown, West Virginia*: SEG

The Wilson, *et al.* paper noted below (deliverable 18) highlights some of the major achievements made during the course of the project and provides an overview of research highlights accepted for publication in the Journal Interpretation. These deliverables include:

- 13) Identification of interactions between two distinct natural fracture sets and their role in reservoir stimulation
- 14) Mapping microseismic energy center distributions
- 15) Identification of horizontal stress gradients
- 16) Development of a novel data-driven process for stress recalibration
- 17) Development of a workflow incorporating iterative stimulation tests on the geomechanical models to obtain agreement between stimulation of the reservoir DFN and stimulation induced microseismic activity
- 18) Compilation of major outgrowths of study into the following paper:

Thomas Wilson, Timothy Carr, B. J. Carney, Jay Hewitt, Ian Costello, Emily Jordon, Keith MacPhail, Adrian Morales, Natalie Uschner, Miranda Thomas, Si Akin, Oluwaseun Magbagbeola, Asbjorn Johansen, Leah Hogarth, and Kashif Naseem, accepted, *Marcellus shale model stimulation tests and microseismic response yield insights into mechanical properties and the reservoir DFN*: The Journal Interpretation, 44P.

Major outgrowths described in the Wilson, *et al.* papers:

- Developed geomechanical model that incorporates local structural elements and all log derived mechanical properties
- Developed basic reservoir DFN using image log data
- Undertook iterative stimulation tests to refine the reservoir DFN and modify geomechanical model parameters to produce observed asymmetric stimulation observed in the reservoir DFN
- Developed workflow to identify variations in the local stress field, the reservoir natural fracture network and their interaction with hydraulic fracture stimulation
- Identified local cross-strike discontinuity along with stress shadowing as possible reasons for asymmetric stimulation
- Identified key geomechanical properties associated with high TOC regions in the Marcellus Shale that can be identified using joint inversion of pre-stack 3D seismic to locate sweet spots in shale gas reservoirs for both exploration and infill well field development

Geomechanical

Table 2.1 shows the computed fracture geometries for newly modeled MIP 3H stages 11 through 20. Figure 2.1 shows the fracture geometry for one of the primary induced hydraulic fractures in stage 20 of well MIP 3H. Figure 2.2 shows the cumulative proppant mass versus time (modeled vs measured), Figure 2.3 shows the slurry volume injected versus time (modeled vs measured), and Figure 2.4 shows the surface pressure versus time (modeled vs measured) for stage 20 of

well MIP 3H. These figures show a good match between the numerical model and the reported data.

Microseismic data was available for all of the stages modeled during this quarter. Microseismic, well, and hydraulic fracture geometric data were visualized in three dimensions. Figures 2.5 through 2.14 show side views of calculated hydraulic fracture geometries and measured microseismic events and magnitudes for stages 11 through 20, respectively, for well MIP 3H. Figure 2.15 shows an overview of all 10 newly modeled hydraulic fracture geometries, microseismic events, and the entire MIP 3H wellbore. Figure 2.16 shows a top view of all newly modeled hydraulic fracture geometries, microseismic events, and the nearby section of the MIP 3H wellbore. Figure 2.17 shows an orthogonal projection of the newly modeled hydraulic fracture geometries, microseismic events, and the nearby section of the MIP 3H wellbore. In Figure 2.5 through Figure 2.14, the measured microseismic events appear to be more prevalent on one side of the MIP 3H wellbore.

Table 2.1: Computed Fracture Geometries – Stage 11 through Stage 20 – MIP 3H

STAGE	Fracture Half-Length (ft)	Fracture Height (ft)	Average Fracture Width (in)
11	631.3	328.8	0.030164
12	649.1	325.2	0.022762
13	597.8	316.2	0.028964
14	552.4	445.8	0.023985
15	740.7	341.9	0.03174
16	660.9	316	0.033038
17	580.4	322.3	0.018099
18	644.1	318.9	0.033231
19	676.1	333.1	0.033314
20	597.2	319.4	0.023954

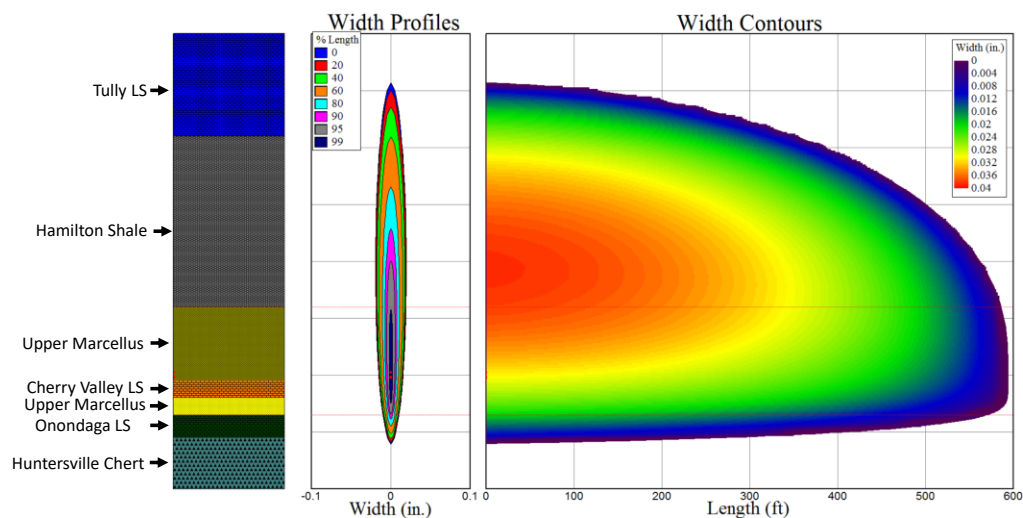


Figure 2.1: Fracture Geometry for Stage 20 - MIP 3H

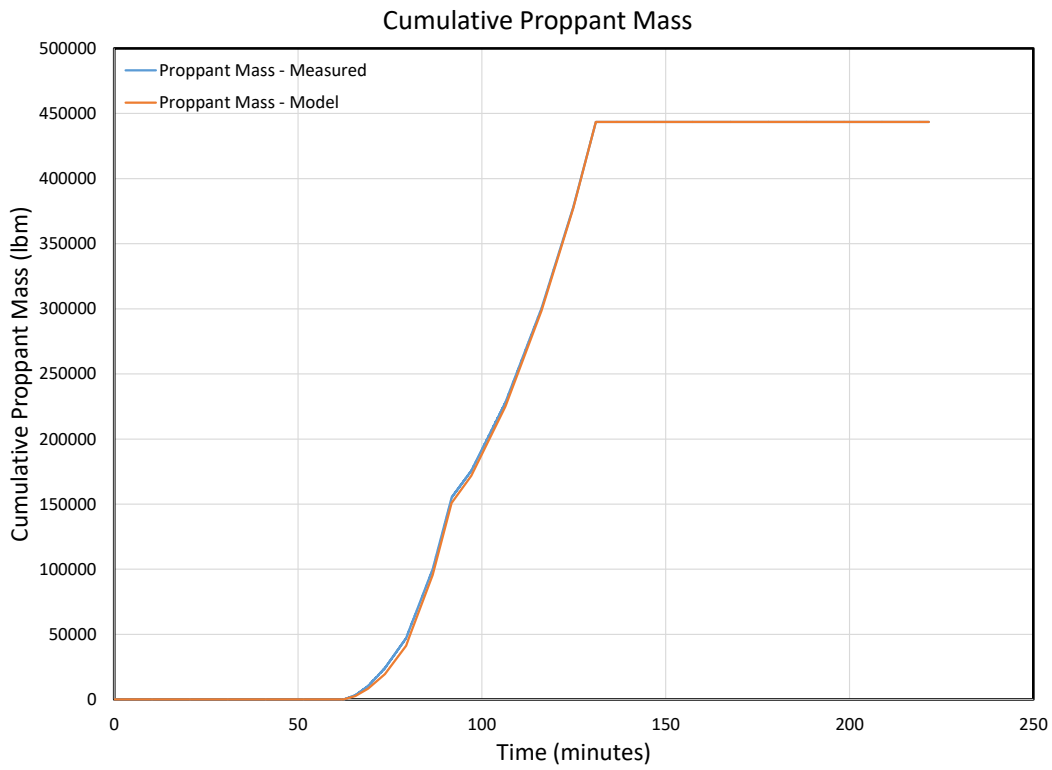


Figure 2.2: Cumulative Proppant Mass for Stage 20 - MIP 3H

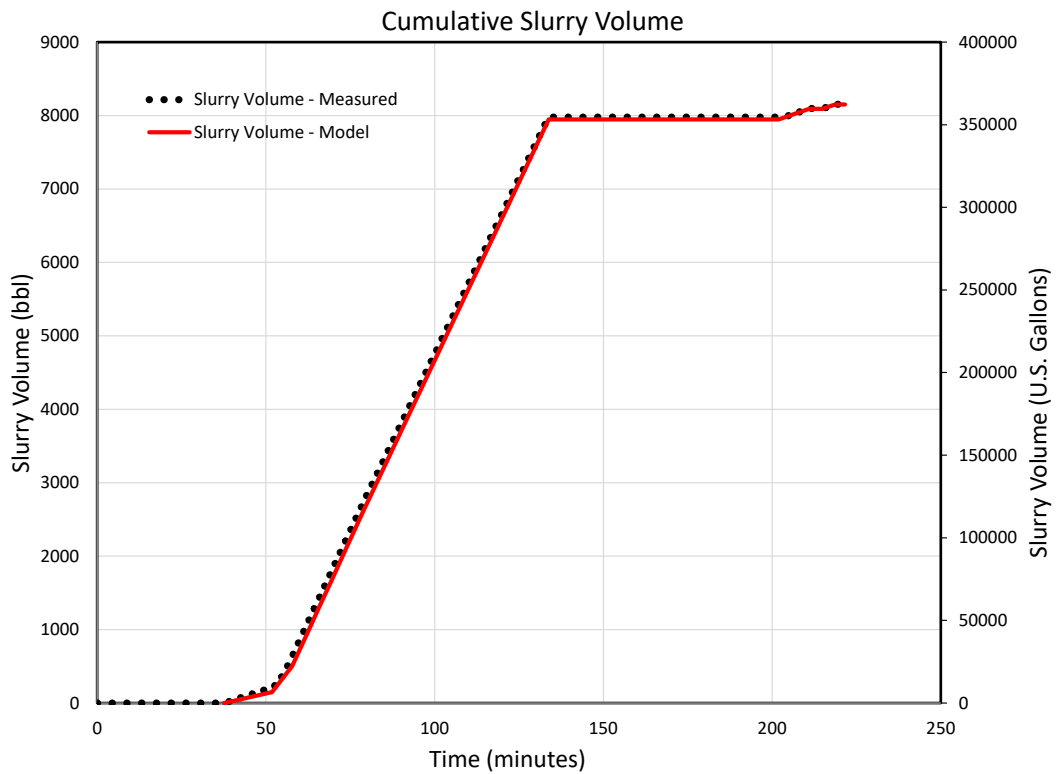


Figure 2.3: Cumulative Slurry Volume for Stage 20 - MIP 3H

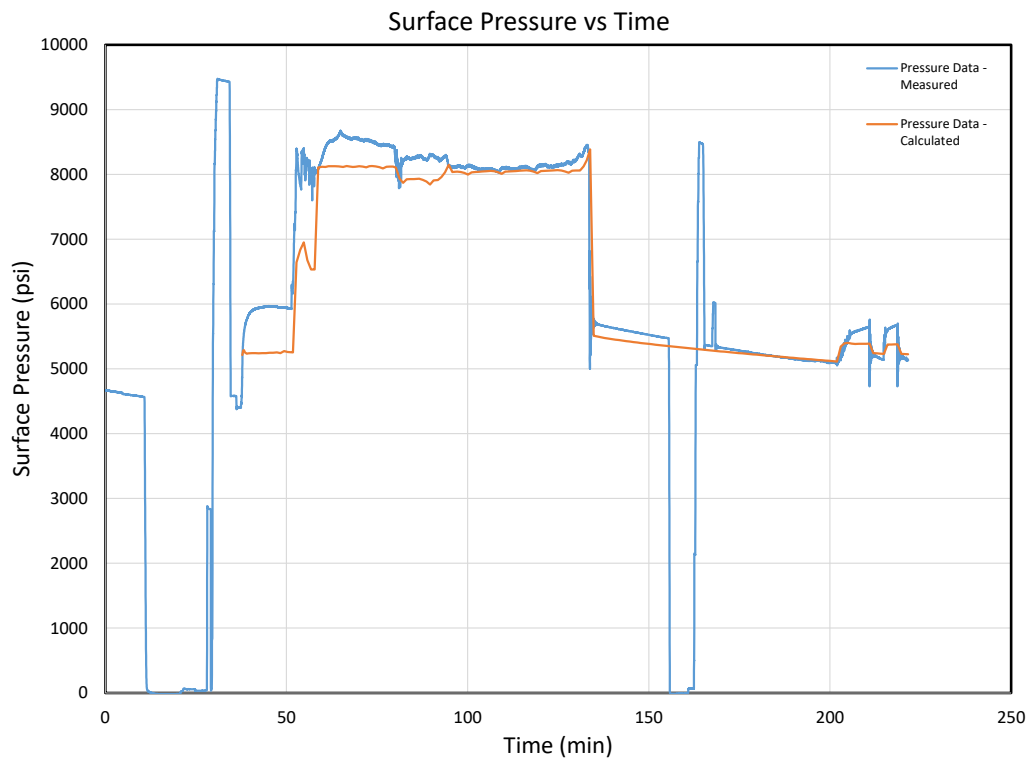


Figure 2.4: Surface Pressure versus Time for Stage 20 - MIP 3H

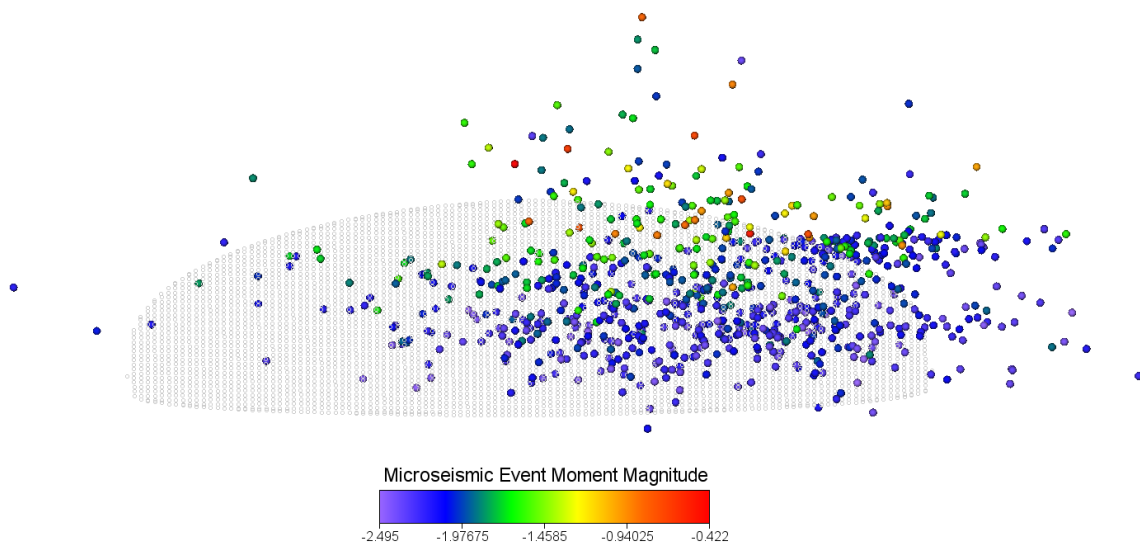


Figure 2.5: Side View of Calculated Hydraulic Fracture and Measured Microseismic Events and Magnitudes for Stage 11 - MIP 3H

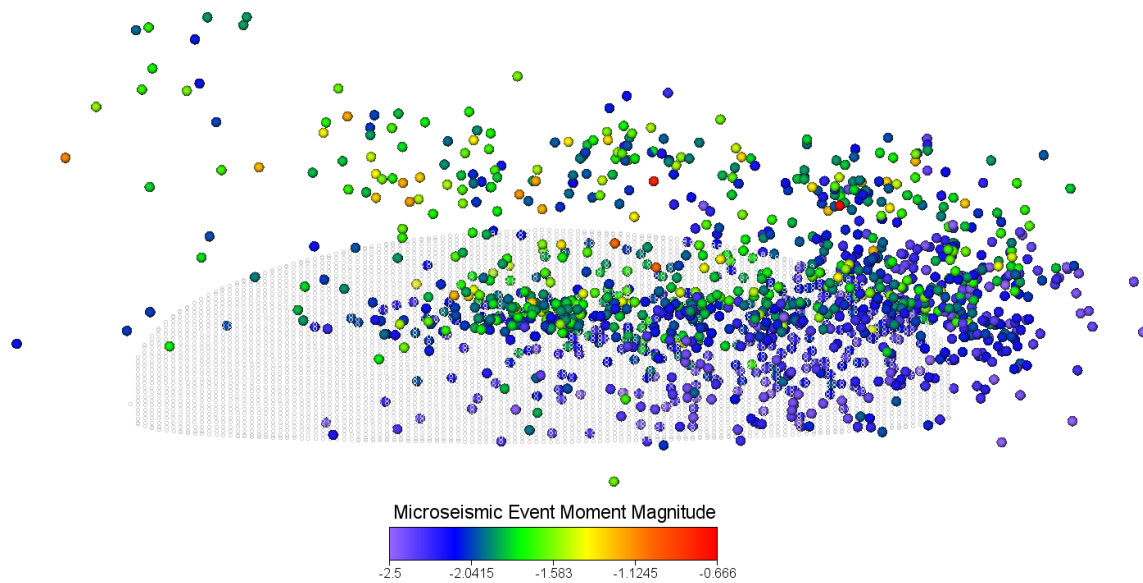


Figure 2.6: Side View of Calculated Hydraulic Fracture and Measured Microseismic Events and Magnitudes for Stage 12 - MIP 3H

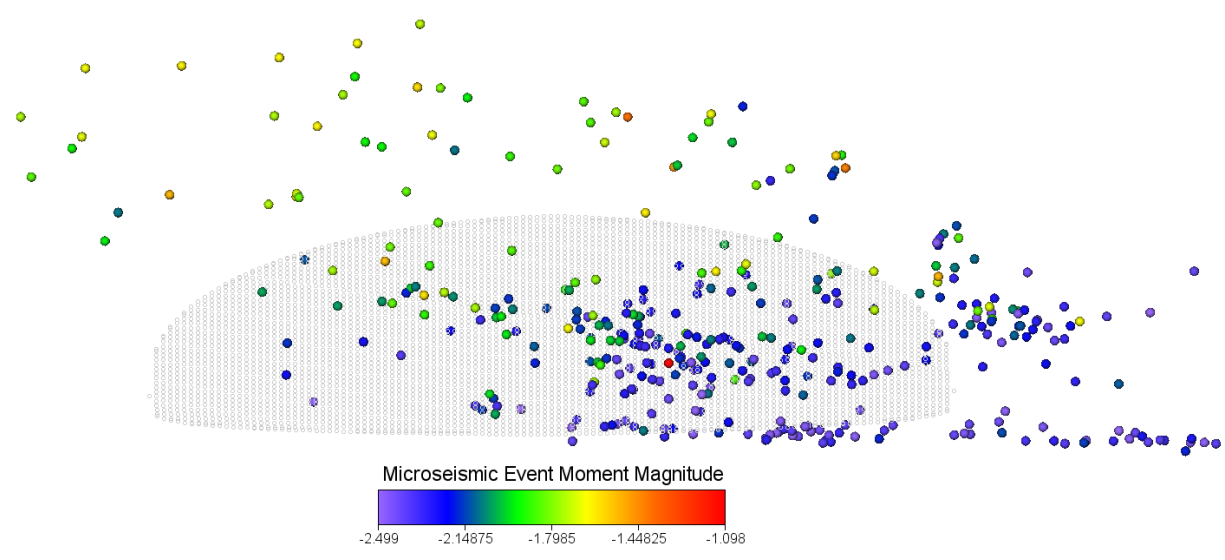


Figure 2.7: Side View of Calculated Hydraulic Fracture and Measured Microseismic Events and Magnitudes for Stage 13 - MIP 3H

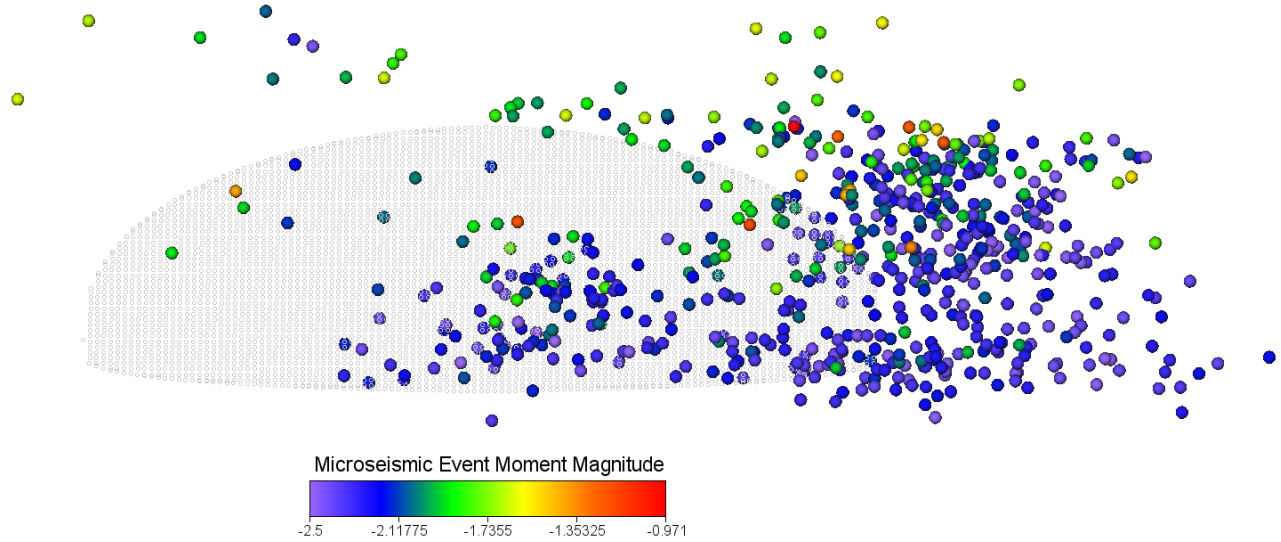


Figure 2.8: Side View of Calculated Hydraulic Fracture and Measured Microseismic Events and Magnitudes for Stage 14 - MIP 3H

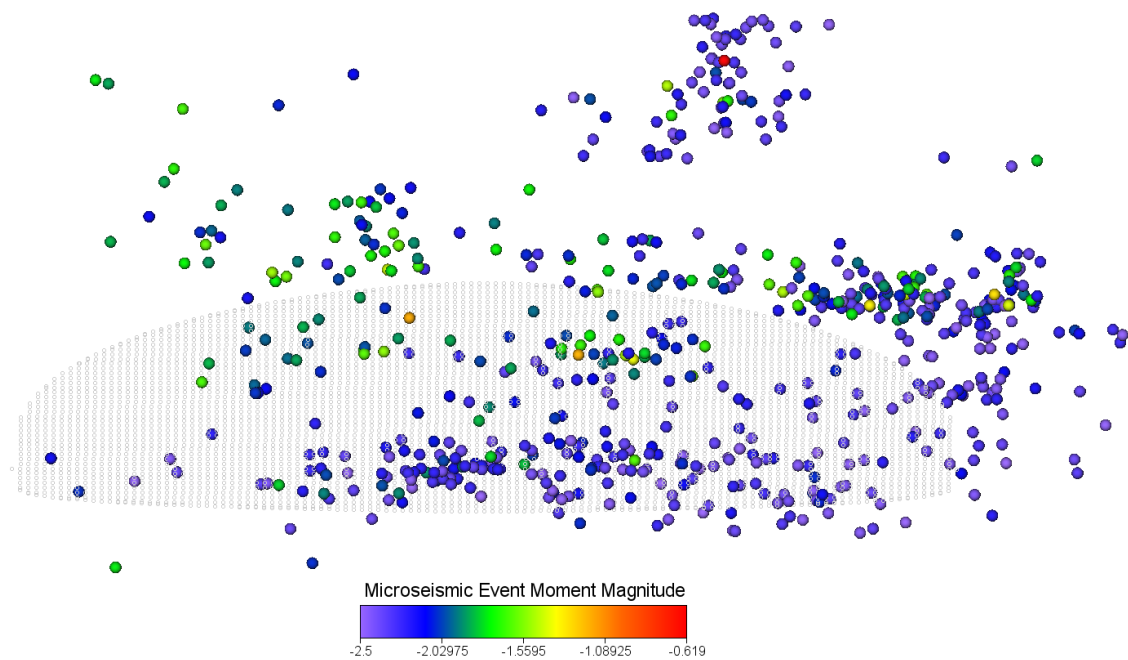


Figure 2.9: Side View of Calculated Hydraulic Fracture and Measured Microseismic Events and Magnitudes for Stage 15 - MIP 3H

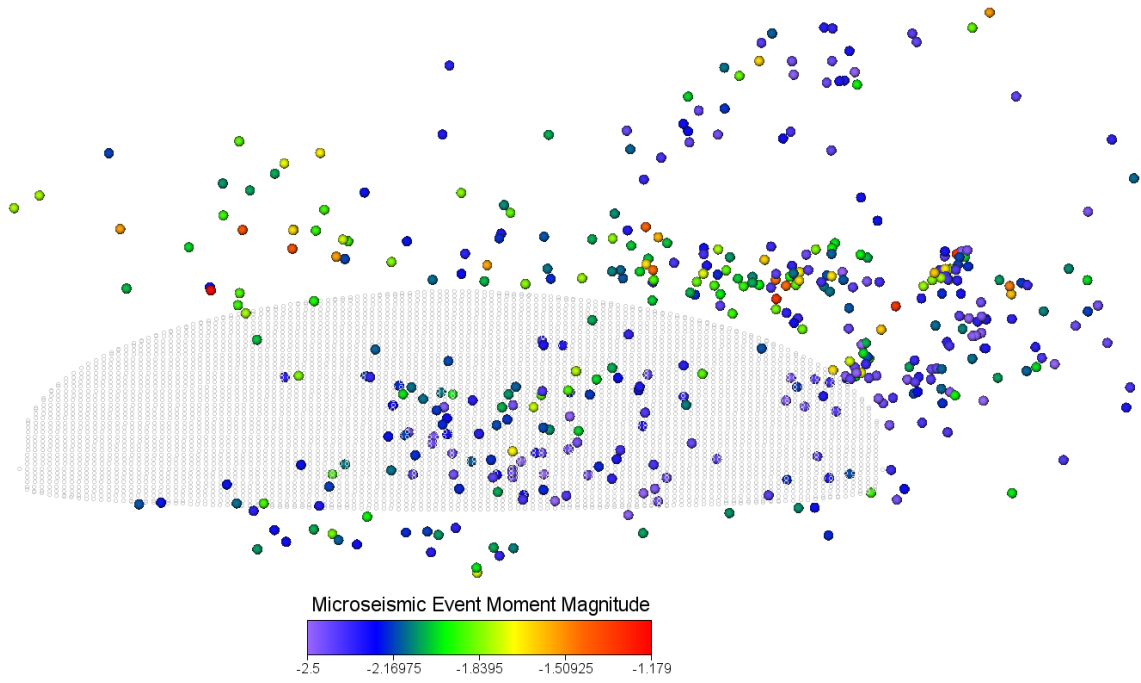


Figure 2.10: Side View of Calculated Hydraulic Fracture and Measured Microseismic Events and Magnitudes for Stage 16 - MIP 3H

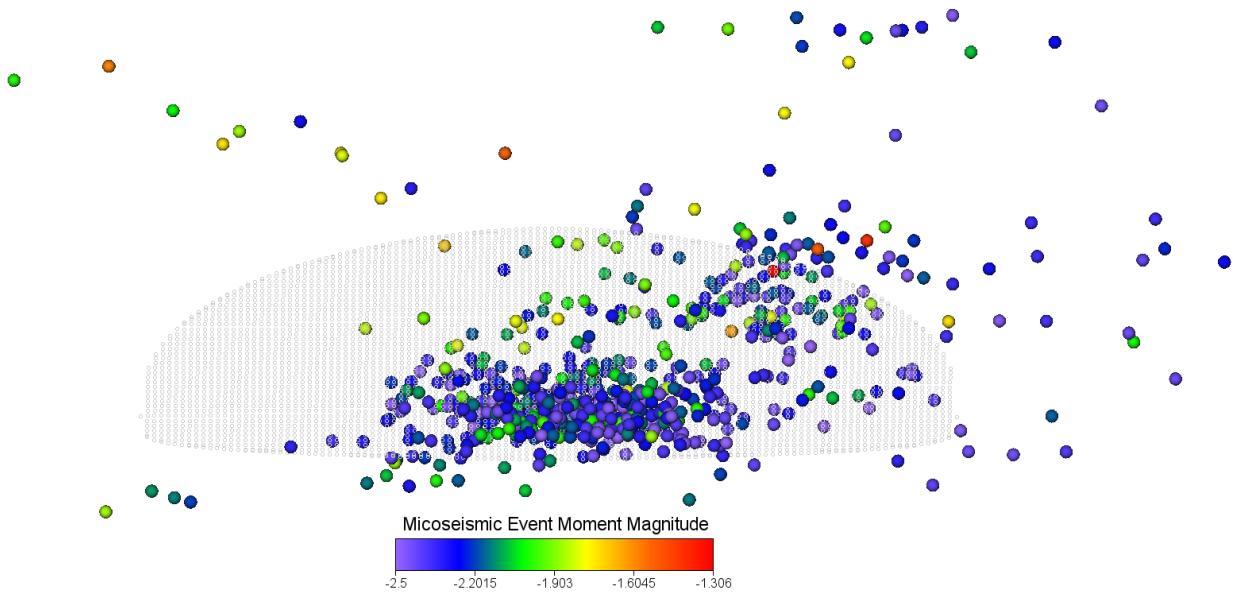


Figure 2.11: Side View of Calculated Hydraulic Fracture and Measured Microseismic Events and Magnitudes for Stage 17 - MIP 3H

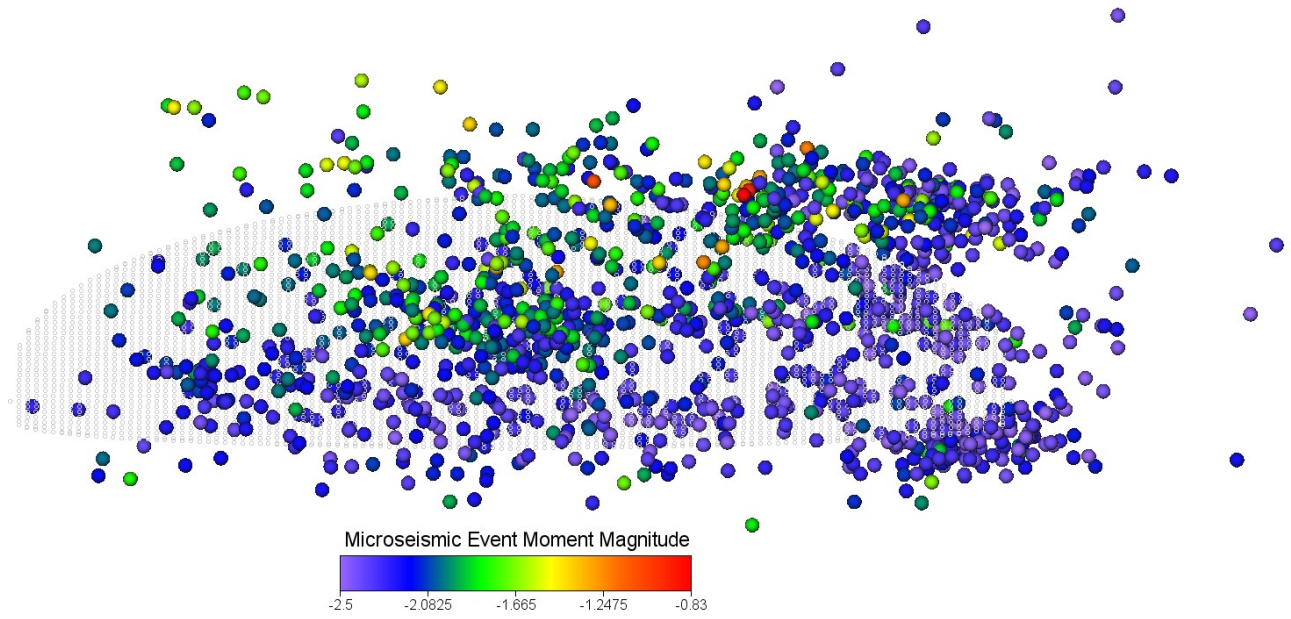


Figure 2.12: Side View of Calculated Hydraulic Fracture and Measured Microseismic Events and Magnitudes for Stage 18 - MIP 3H

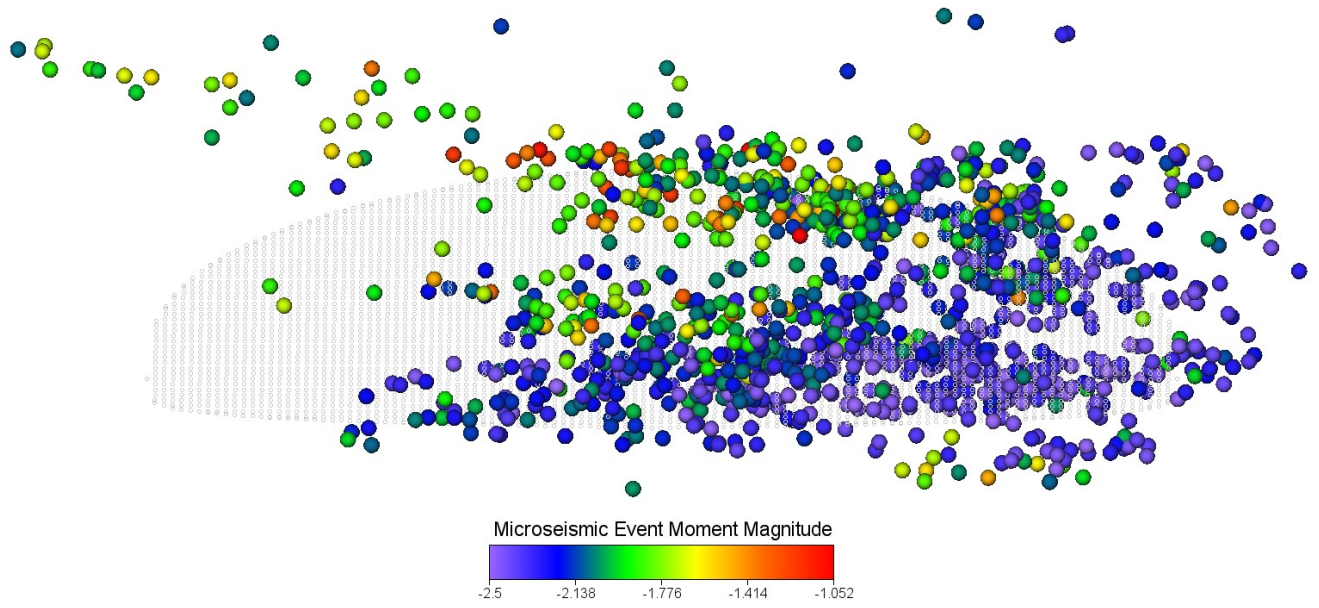


Figure 2.13: Side View of Calculated Hydraulic Fracture and Measured Microseismic Events and Magnitudes for Stage 19 - MIP 3H

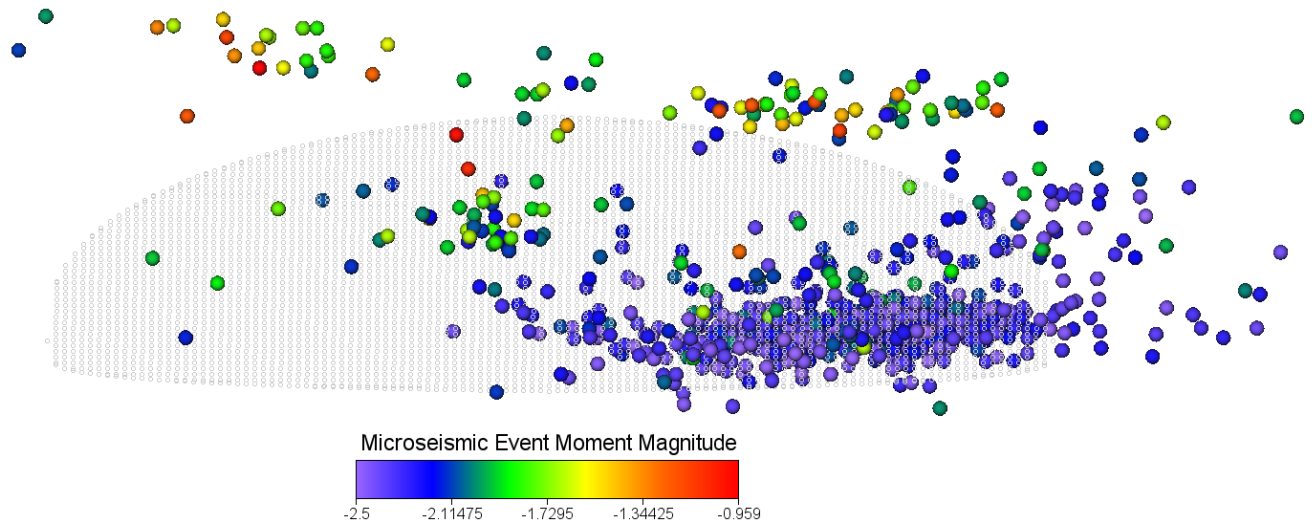


Figure 2.14: Side View of Calculated Hydraulic Fracture and Measured Microseismic Events and Magnitudes for Stage 20 - MIP 3H

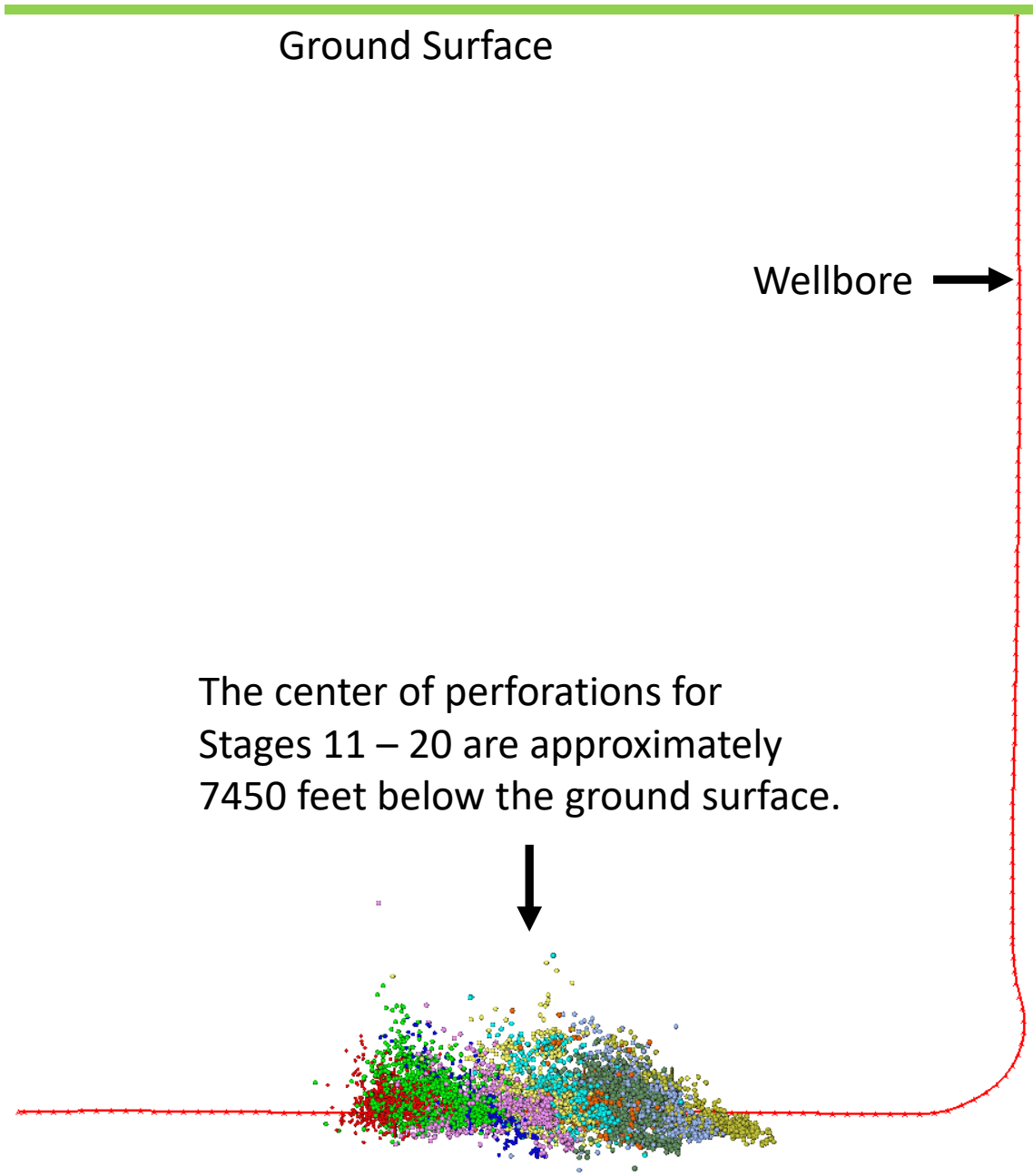


Figure 2.15: Overview of Calculated Hydraulic Fracture Geometries, Measured Microseismic Events, and Entire Wellbore for Stage 11 through Stage 20 - MIP 3H

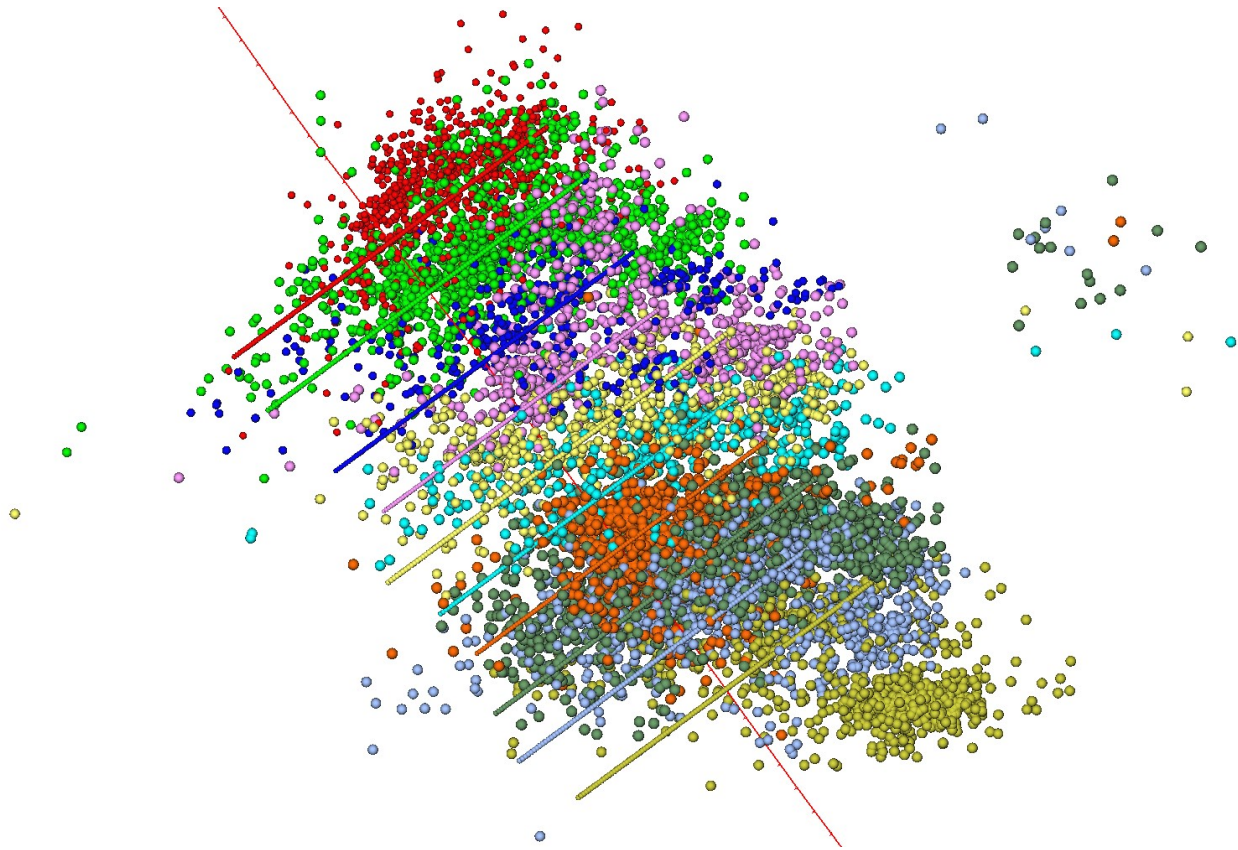


Figure 2.16: Top View of Calculated Hydraulic Fracture Geometries, Measured Microseismic Events, and Nearby Wellbore for Stage 11 through Stage 20 - MIP 3H

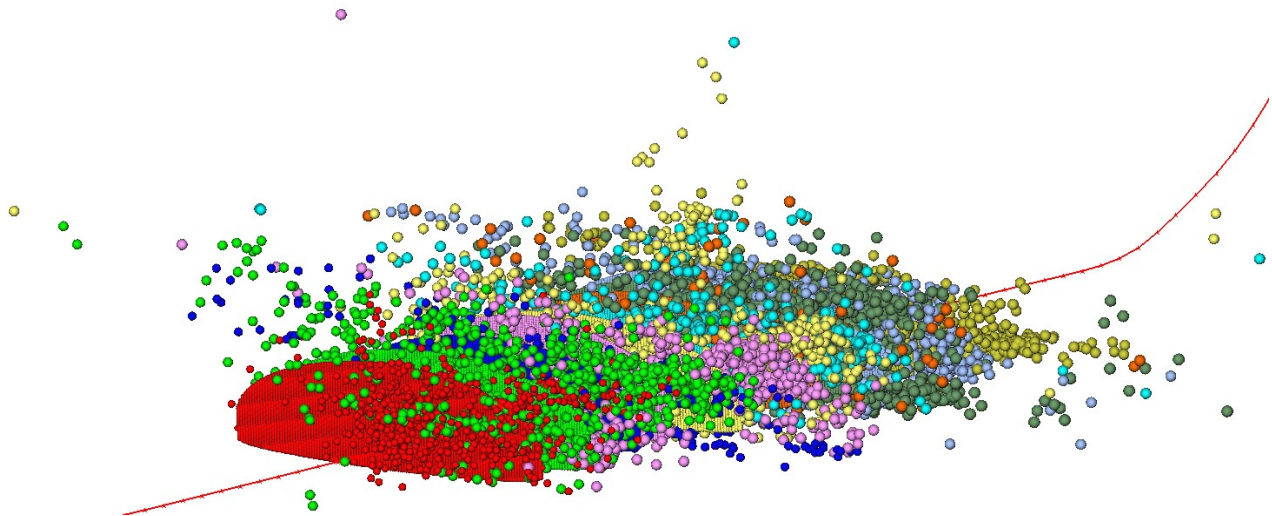


Figure 2.17: Orthogonal View of Calculated Hydraulic Fracture Geometries, Measured Microseismic Events, and Nearby Wellbore for Stage 11 through Stage 20 - MIP 3H

Unconventional Fracture Model (UFM) Approach

An unconventional fracture model (UFM) which accounts for the natural fractures orientations within the Marcellus Shale was generated using the image and geomechanical logs from the 3H, and the completion and microseismic data for 3H and 5H. Pre-existing natural fractures interpreted from the image logs were used to generate a discrete fracture network (DFN). An UFM approach is utilized to simulate multi-stage complex hydraulic fracture geometry estimation. As a result fractures are not symmetric planar fractures on both sides of the well bore (Figure 2.18). This approach combines geomechanics with natural fracture interactions for hydraulic fracture geometry estimation.

A close match of simulated hydraulic fractures with microseismic data was obtained by introducing horizontal stress anisotropy and horizontal stress gradient. The resulting model is capable of simulating the reservoir production history. We demonstrate that UFM approach is capable of representing a more realistic model of the propagated hydraulic fractures in presence of multiple sets of natural fracture network. It also matches the microseismic trends, which is not possible to achieve using planar fracture models.

Finally, production simulation was performed under rate control mode while matching bottom hole pressure and water production rate for the two wells in an unstructured grid reservoir model. The history matched production for two horizontal wells in Marcellus Shale (Figures 2.19 and 2.20). The developed model can be used to optimize production for the current wells and also provides a tool for future well placement as well as well spacing optimization in the area.

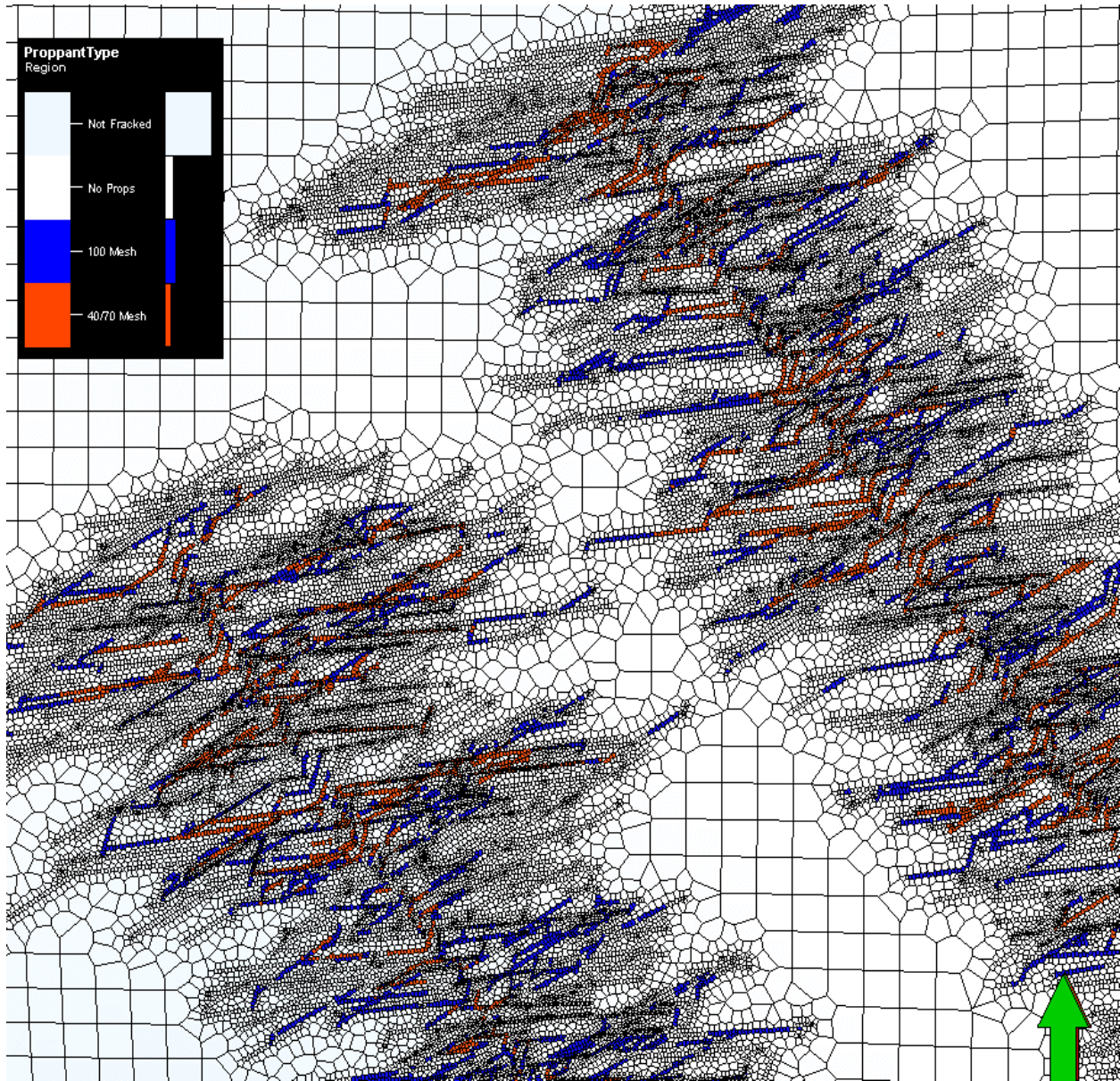


Figure 2.18: Modeling of asymmetric planar fractures about well bore, MIP 3H and 5H

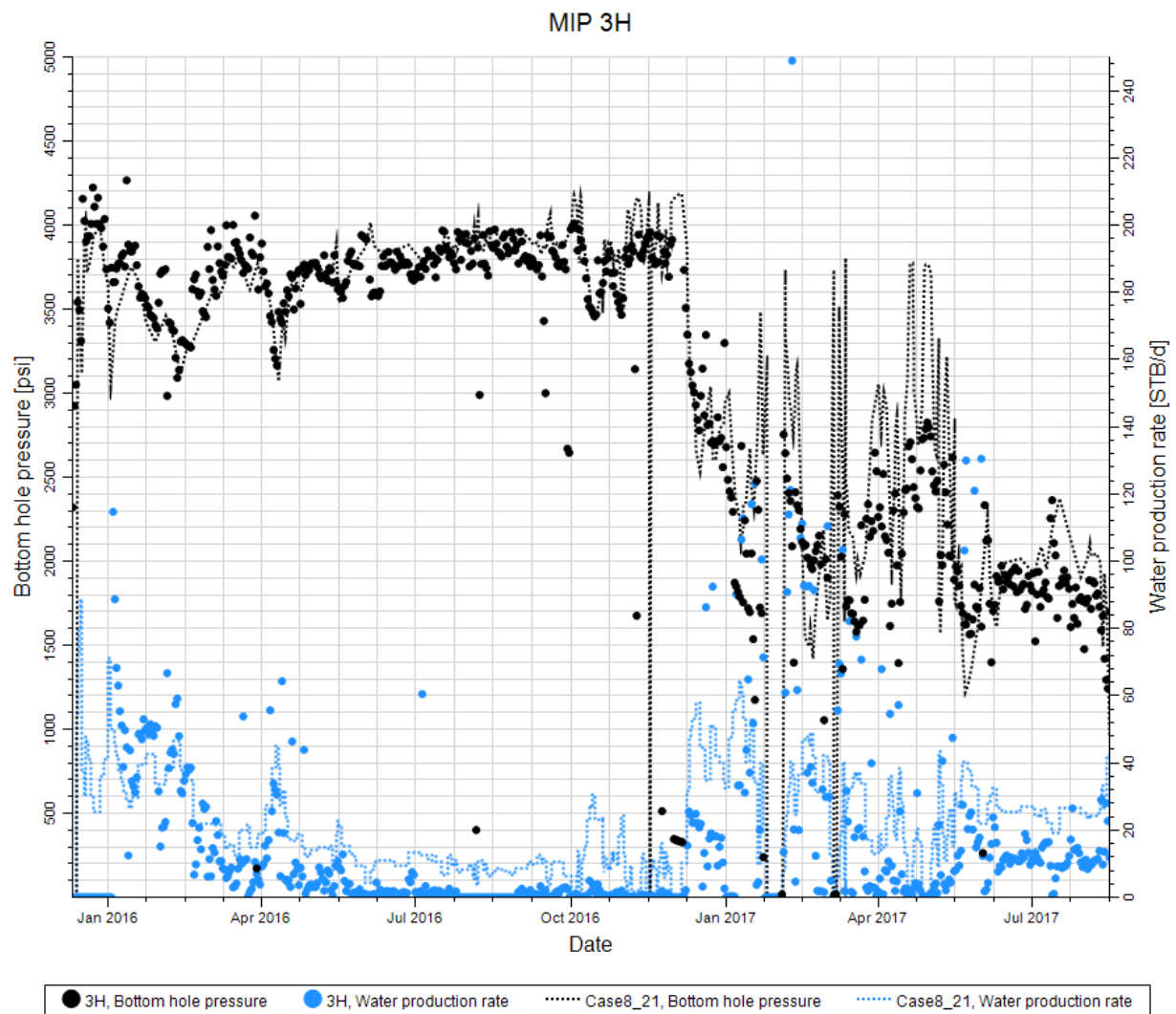


Figure 2.19: Simulation of Bottom Hole Pressure and Water Production MIP 3H

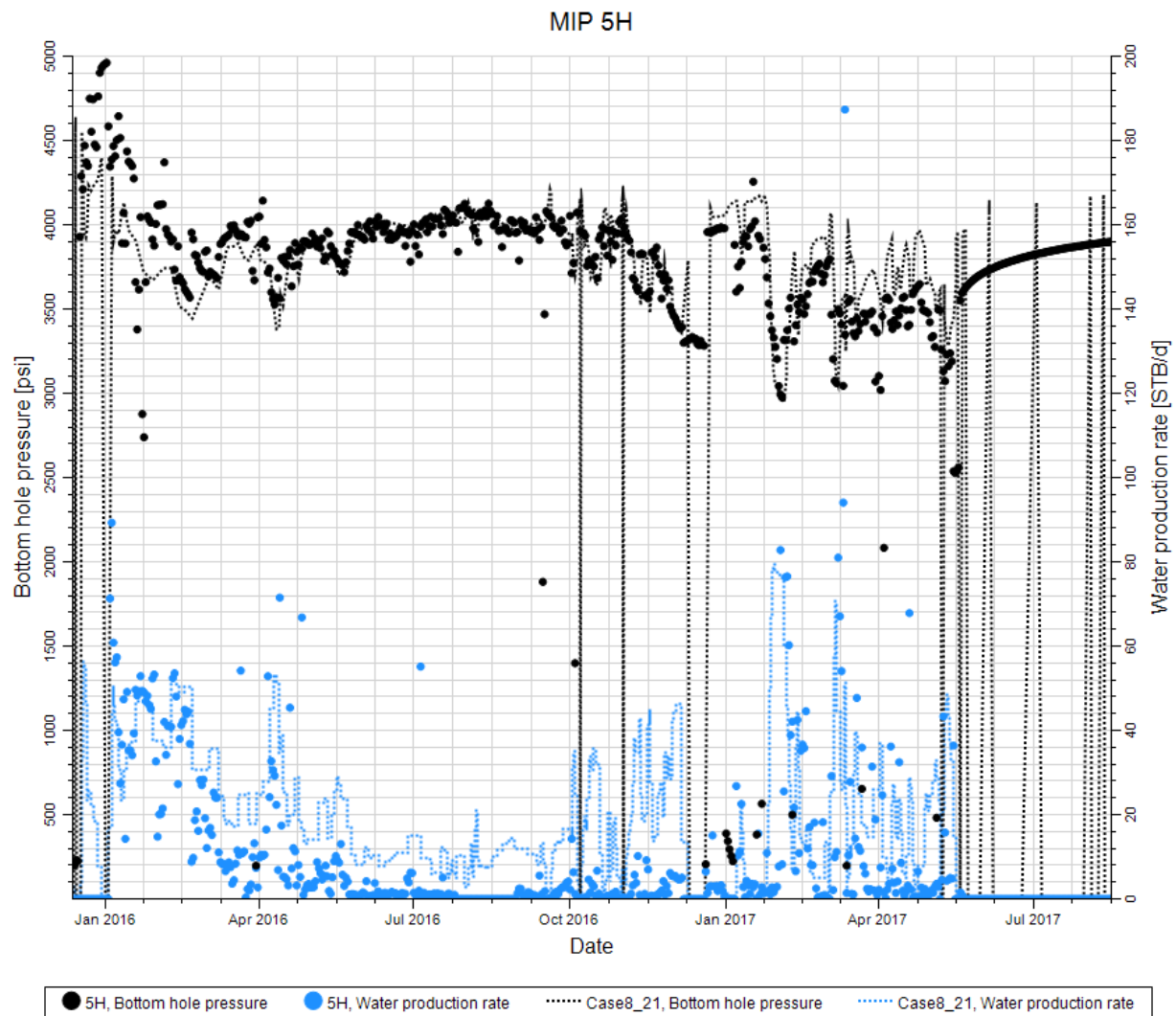


Figure 2.20: Simulation of Bottom Hole Pressure and Water Production MIP 5H

Products

1) Presentation of paper at 2017 Annual International SEG meeting:

The paper titled “*Relationships of $\lambda\rho$, $\mu\rho$, brittleness index, Young’s modulus, Poisson’s ratio and high TOC for the Marcellus Shale, Morgantown, West Virginia*” by Thomas H. Wilson*, Payam Kavousi, Tim Carr, West Virginia University; B. J. Carney, Northeast Natural Energy LLC; Natalie Uschner, Oluwaseun Magbagbeola and Lili Xu, Schlumberger, was presented at the annual SEG meeting, this past September in Houston, TX.

The paper was forwarded with the previous quarterly

Plan for Next Quarter

Geophysical

All milestones have been met. Continuation is possible as needed.

Geomechanical

The modeling study will continue. The team will investigate other stimulation stages at well MIP 3H through the use of available information on the hydraulic fracturing field parameters (fluid volumes, pumping rate, proppant schedule, and geophysical data). Results presented in this report show that the computed fracture heights are higher than those which were computed without discrete fracture networks, and are closer to the height of the microseismic data cloud. The analysis of microseismic data will continue and a comparison of fracture geometries will be made with available microseismic data.

Topic 3 – Deep Subsurface Rock, Fluids, & Gas

Approach

The main focus of the subsurface team led by Sharma this quarter was to analyze core, fluid and gas samples collected from the MSEEL site. Members of Sharma's lab group (Dr. Warriar and Mr. Wilson) and Dr. Hanson from Mouser's lab group continue to coordinate and supervise all sample collection. Samples were also distributed to the research team at OSU and NETL for analysis under different sub-tasks. Several talks and presentations were given at local and regional conferences /universities.

Results & Discussion

Progress on Sidewall Core, Vertical Core & Cutting Analysis

The side wall cores are curated at OSU and WVU. Based on the geophysical logs, eight samples were selected from different lithologies, i.e. zones, where the team expects to see maximum biogeochemical variations. Samples were homogenized and distributed among different PI's and are currently being processed for biomarkers, isotope analysis, elemental analysis, porosity/pore structure, and noble gas analysis. For whole core analysis, cores were taken from 1-foot intervals through the 111 feet of whole vertical core. Samples were ground, homogenized, and distributed to different groups at WVU, OSU, and NETL for different analysis.

In **Sharma's Lab**, Ph.D. student Rawlings Akondi completed a manuscript focused on understanding the relict or non-viable microbial community composition in the side wall cores.



Figure 3.1: Relative abundance of lipid biomarker functional groups for the Mahantango, Marcellus top, and upper Marcellus Shale formation.

The manuscript has been sent to co-authors for review and then to be submitted to journal *Geomicrobiology*. Results show that the highly impermeable, thinly laminated, gray-to-black-colored, organic-rich Marcellus Shale formations showed much less lipid biomass and variety compared to the thickly-laminated, silt-sand-shale interbedded Mahantango formation of higher permeability and less organic matter content. This is a plausible indication of higher paleo microbial activity in this zone. Biomarkers indicative of stress such as trans fatty acids and oxiranes were present in the cores, a potential indication that the cores had experienced some amount of stress (**Figure 3.1**). This study will shed more light on how factors like paleo environment, thermal history,

and organic matter source and permeability can affect the distribution of microbial lipid biomarkers in the deep subsurface geologic formations. Presently, Rawlings is preparing figures and organizing the structural framework for a manuscript that will be focused on interpreting the compound-specific isotope composition of the lipid biomarkers, along with the bulk organic carbon isotopic values, as well as the major elemental geochemical analysis.

Another Ph.D. student in **Sharma Lab**, Vikas Agrawal, analyzed the data generated from ^{13}C solid state NMR of the kerogen samples extracted from Mahantango and different zones of Marcellus shale at the MSEEL site using the software *TopSpin*. The NMR analysis was done to determine the fractions of different aliphatic and aromatic structural parameters of kerogen. The analysis shows that the kerogen from Mahantango and different zones of Marcellus is dominated by aromatic carbon ranging from 86% to 92%, and there appears to be no significant variation in the total percentage of aromatic vs aliphatic carbon in different units. However, analysis of fractions of different functional groups within the aliphatic and aromatic fractions show some differences (**Figure 3.2**) especially in lower Marcellus shale unit. Lower Marcellus has higher fraction of non-protonated aromatic bridgehead and lower fraction of protonated aromatic carbons as compared to other units. This is probably because lower Marcellus received higher influx of marine organic matter during deposition. Since marine organic matter is rich in aliphatic carbon chains, these aliphatic chains might have broken down on maturation form free radicals that recondensed to form bridgehead carbon atoms. Vikas also went to GFZ Potsdam, Germany to perform open and closed system pyrolysis experiments on a few kerogen samples. Data analysis and interpretation of the pyrolysis results is in progress.

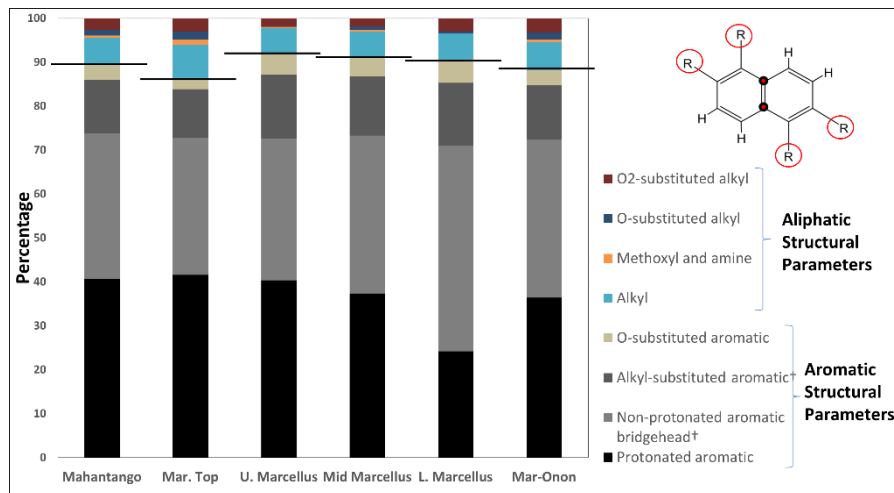


Figure 3.2: Aliphatic and aromatic structural parameters determined from ^{13}C solid state NMR analysis of kerogen sample from Mahantango and different zones of Marcellus shale at the MSEEL site.

In **Cole's** Lab, large field backscattered electron (BSE) maps have been acquired for all 8 polished thick sections of MSEEL sidewall core. These core were split and shared among the Cole-Darrah-Wilkins labs at OSU. These data allow large-area analysis of mineralogy/rock fabric/organic matter (OM) associations within this diverse suite of samples. An example low-magnification BSE image used to construct such a map is shown in **Figure 3.3**; sample **MO 1** (Lower Marcellus- In Onondaga Limestone transition, depth 7552').

QEMSCAN mineral maps (several 1 mm^2 fields) also have been measured for the same 8 thick sections. Quantification of modal mineralogy is ongoing. Sample **MT 30** (Mahantango, depth 7440') is shown in Figure 3.4. This sample is similar to sample **MT 25** (Marcellus Top, depth 7451') both in mineralogy and texture (both are illitic clay and quartz-rich with a tight fabric), although Marcellus Top sample is richer in pyrite and OM than the Mahantango sample. Rietveld analysis of XRD data acquired from powdered core (to determine semi-quantitative mineralogy in weight percent) has commenced. Lower Marcellus, 7543' (**ML 10**) Rietveld analysis was uploaded to the MSEEL data portal. Other XRD data and SEM images also were uploaded, per request, prior to the MSEEL External Advisory Committee Meeting.

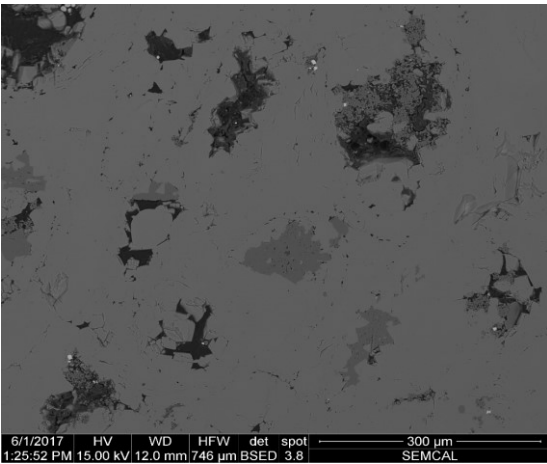


Figure 3.3: BSE image of MO 1 (Lower Marcellus-Onondaga Limestone transition, depth 7552'). Horizontal field width is approximately $\frac{3}{4}$ mm. In this sample, OM (darkest material) is associated with ooids (oval-shaped features) in the centers and along grain boundaries. Some of these ooids are filled with minerals that appear to be replacing OM, and may reflect remnant pore fluid chemistry.

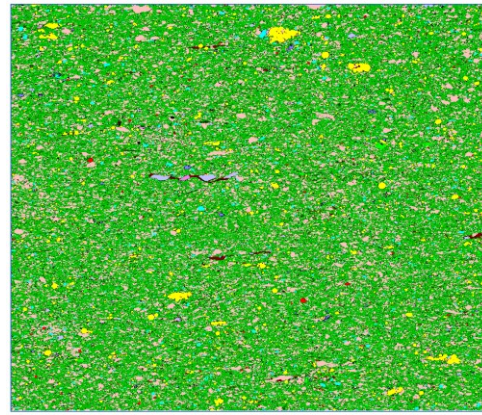


Figure 3.4: QEMSCAN mineral map of 1 mm² region of MT 30 (Mahantango, depth 7440'). Green matrix is composed mainly of illitic clay (58.2 %); pink is quartz (25.4 %); yellow is pyrite (3.1 %); cyan is albite (1.9 %); dark green is muscovite mica (0.9 %); OM is maroon (0.4%, shown by red arrow), light green is Fe-chlorite (1.5%), red is titania (0.5 %); lavender is calcite (0.4 %). Minor apatite (0.1%, shown by pink arrow associated with OM) and dolomite (0.1%) also are detected, and unclassified mixed pixels are black (7.0 %). Titania (anatase or rutile) will require cross-checking for barium (barite), due to overlap of EDXS spectral lines for

In **Darrah's Lab**, the analyses of sidewall, vertical cores, and to a lesser extent drill cuttings, have been the primary task in the last quarter. The team has analyzed trace elements (U, Th, K) in a suite of samples from both wells. Additionally, they have also analyzed the trace element composition of vein-filled fractures observed within two sidewall core samples. The major focus during the last month has been the analyses of radiogenic and nucleogenic helium-4, neon-21, argon-40, and xenon-131; 134; 136 isotopes in the solid samples by step-wise heating and fusion. These data will represent the first analyses of these isotopes in pristine samples to be reported in the literature. Preliminary work suggests spatial differences in diagnostic radiogenic noble gas ratios ($^4\text{He}/^{21}\text{Ne}^*$, $^4\text{He}/^{40}\text{Ar}^*$) according to the distance from observed fractures. Ongoing work will develop these analyses to help improve bottom-up estimates of reservoir stimulation volumes by combining the produced fluid and solid noble gas data.

Progress on Produced Fluid and Gas Analysis

Produced water samples were collected in 5-gallon carboys in mid-August. The samples were transported, filtered and processed in Sharma Laboratory at WVU. All water samples were collected in different containers using different methods/ preservatives etc. specified for different kinds of analysis. All PI's at OSU and NETL were provided detailed sampling instructions. Graduate students John Pilewski and Vikas Agrawal at WVU, and Dr. Andrea Hanson from OSU, were primarily in charge of sample collection and distribution among different PI's at WVU, OSU, and NETL. The collected fluids are currently being processed for biomass, reactive chemistry, organic acids, and noble gas and stable isotope analysis at different institutes.

Sharma Lab continues to analyze O, H, and C isotopic composition of produced fluids collected from 3H and 5H. The carbon isotope composition of the dissolved inorganic carbon in the produced water continues to show the enrichment in ^{13}C with $\delta^{13}\text{C}_{\text{DIC}} > +17 \text{‰ V-PDB}$. The

isotope analysis of input fluids, sand, cement, reservoir rock and carbonate veins strongly support the microbial utilization of lighter carbon (^{12}C) by methanogenic bacteria in the reservoir. This indicates that introduction of C containing nutrients like guar, methanol, methylamines, etc. could stimulate certain methanogen species in the reservoir to produce biogenic methane in the reservoir. Sharma Lab has also analyzed the carbon isotope signature of produced methane and CO_2 from the produced gas in MIP 3H and 5H. Although the concentration of CO_2 is fairly low in produced gas it does show an increase in $\delta^{13}\text{C}$ signature over time supporting possibility of microbial utilization of $^{12}\text{CO}_2$.

In **Cole's Lab**, analysis of fluid samples from the MIP 3H and 5H wells continues. Fluid samples have been analyzed for anions, and prepared for major and trace metal analysis by ICP OES and ICP MS. Analysis of precipitates and colloidal material, pipetted from the bottom of containers of flowback and filtered (both fresh and year-old brine samples from the 3H well) has commenced. The major Fe-phase is akaganeite (determined from both XRD and SEM analysis of the filters). Synthetic fluids also were prepared in the lab to mimic acid mine discharge (AMD) of variable concentrations, and mixed with flowback fluids from well MIP 3H. ICP-MS of supernatant fluid and XRD/SEM analysis of the precipitates is underway to determine whether precipitates formed in the mixtures would uptake trace metals.

In **Wilkins Lab**, isolate genome sequences have been generated for six new microbial cultures, representing species within the *Halanaerobium*, *Orenia*, and *Marinilabilia*. 16S rRNA gene analyses of MSEEL produced fluids have revealed members of these taxa dominating the microbial down-hole populations over extended periods of time. Both the isolate genomes and the cultures are available for public use upon request. Genomes are available at JGI IMGs resource: <https://img.jgi.doe.gov/cgi-bin/pub/main.cgi>. *Halanaerobium* strains are found to dominate microbial populations in deep shales, including the MSEEL wells. Analysis of a *Halanaerobium* strain has revealed metabolic changes when the culture is incubated under pressures characteristic of deep shale environments. Using nuclear magnetic resonance to analyze *Halanaerobium* metabolites, a graduate student in the Wilkins Lab (Anne Booker) revealed significant changes in intra-cellular carbon flux – and subsequent secretion of fermentation end products – when cells are grown at 5000 psi (**Figure 3.5**). The increased per-cell production and secretion of organic acids under pressurized conditions has implications for down-well corrosion of steel infrastructure. A manuscript detailing this work is expected to be submitted in December 2017. In a prior report, we reported increased *Halanaerobium* cell attachment on quartz surfaces in response to pressurized conditions. New experiments are currently ongoing to investigate the attachment of cells onto fresh shale surfaces, which will be imaged using SEM.

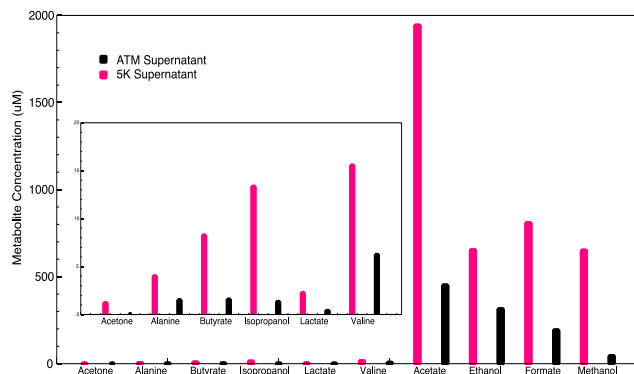


Figure 3.5. Per-cell metabolite concentrations (10^6) for *Halanaerobium* cells grown at atmospheric pressure and at 5000 psi. Clear increases in concentrations of acetate, formate, and methanol are apparent in biomass grown under pressurized conditions. Results are the average of three biological replicate cultures for each condition

In **Wrighton's Lab**, DNA extractions from all produced fluid samples (last sample collection: August, 2017) have been completed on all MSEEL samples. Samples for 16S rRNA iTag and metagenomic sequencing will be submitted on Wednesday, October 25th. This data will not only support publications in the Wrighton laboratory, but also contribute to research led by Mouser and Wilkins. They have received 16S rRNA iTag data for produced fluid samples through April 2017 and are in the process of analyzing the data. All MSEEL samples collected through August 2017 have been submitted to Pacific Northwest National Laboratory, Environmental Molecular Sciences Laboratory for metabolite analyses of produced fluids.

In the **Mouser's Lab**, significant progress has been made in identifying and quantifying the intact bacterial lipids in the MIP 3H produced water (**Figure 3.6**). Temporal trends in microbial biomass in the flowback and produced water (**Figure 3.6c**) revealed a predominance of bacterial phospholipids and unique glycophospholipids containing anionic, glycosylated, and tentatively identified acylated head groups (**Figure 3.6a**). These glycosylated head groups are unique structures and appear to be associated with other halotolerant bacteria. As a result, these specific glycophospholipids may serve as chemotaxonomic biomarkers for heterotrophic, halotolerant bacteria residing in highly saline fluids retained in terrestrial environments. Furthermore, modified acyl-ether core lipid structures (**Figure 3.6b**) were tentatively identified in some produced water samples; these acyl- ether core structures are thought to be synthesized only by anaerobic bacteria, providing another taxonomic biomarker for bacteria in produced water. They analyzed lipids in produced water from MIP 3H after the production logging in early 2017 (Days 462 and 490); the relative abundance of lipid classes (**Figure 3.6c**) suggests the microbial biomass composition adjusted quickly despite the extensive well disturbance. Considering fluid bulk geochemistry and the consistent high abundance of these lipid head groups, we surmise these lipid structures contribute to the stability of cellular membranes under osmotic stress, the selectivity of membrane permeability, and play a role in the stabilization of membrane proteins.

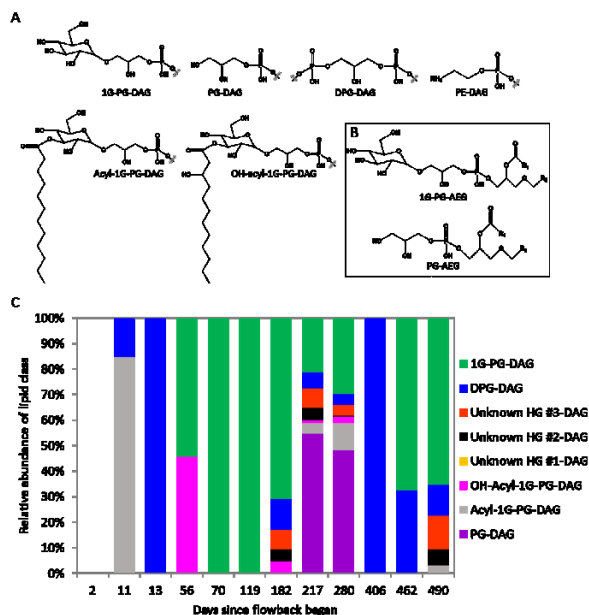


Figure 3.6. Detected lipid classes and temporal abundance in flowback and produced water. A) detected lipid head groups (only the head groups are shown; the dashed line indicates the head group is bound to a diacylglyceride core); **B)** detected lipid structures containing an acyl-ether core structure; and **C)** temporal abundance of detected lipid classes in flowback and produced water (the relative abundance is based on a calculated lipid concentration determined using hydrophilic liquid interaction chromatography coupled to a quadrupole-time-of-flight mass spectrometry system operated in positive ion mode). Mode, therefore, is not included in panel C.

Darrah's Lab continued time-series analysis of fluid samples collected monthly from the MIP 3H and 5H wells. However, the major focus of the time-series and fluids analyses has transitioned from sample analyses to data interpretation and publication in the last quarter. The time-series analysis continues to show a trend of increasing elemental fractionation of noble gases, specifically

heavy noble gases. Preliminary interpretations of data suggest that the physical locations that source hydrocarbon gases and brines changes over time and that heavier noble gases can be used to de-convolve the physical location of hydrocarbon and brine fluid production over time. The team is in the process of preparing a manuscript based on this data (Darrah, Moortgat, Cole, Sharma, *et al.*, with anticipated submission to *AAPG Bulletin*) that will be integrated with numerical modelling (Moortgat at OSU) to improve fluid recovery potential models. This work was also the basis of a pending proposal to NETL/DOE. While the time-series analyses reveals that fluids are produced from different physical locations within the shale matrix (fractures, desorption from organic matter, brine, clays), helium isotope and xenon isotope data indicate that there is a consistent source of resolvable, exogenous mantle-derived fluids present within the gas throughout fluid sampling. This data is a source of a second manuscript in preparation for *Geochimica et Cosmochimica Acta* (Grove, Darrah, Cole, Sharma *et al.*) that documents these mantle sources and integrates noble gas data within the context of other data from the Appalachian Basin. In addition to helping to constrain the source of exogenous natural gases, radiogenic and nucleogenic noble gas isotopes: helium-4, neon-21, argon-40, and xenon-131; 134; 136 measured in produced fluids have been used to estimate the timing of hydrocarbon generation and the residence of fluid isolation within the Marcellus Shale. Current estimates suggest that the hydrocarbon fluids produced from the 3H and 5H wells have been isolated within the Marcellus Shale for at approximately 326 ± 11 Myr following methods recently developed in publications by Holland *et al.*, 2013; Barry *et al.*, 2017. These findings are the basis for a third manuscript in preparation (Darrah, Cole, Sharma) in preparation for *Geology*.

Products

Isolate genome sequences have been generated for six new microbial cultures, representing species within the Halanaerobium, Orenia, and Marinilabilia. 16S rRNA. Both the isolate genomes and the cultures are available for public use upon request. Genomes are available at JGI IMGs resource: <https://img.jgi.doe.gov/cgi-bin/pub/main.cgi>

Several manuscripts are in preparation.

Plan for Next Quarter

Sharma's Lab

Data analysis and interpretation of the pyrolysis results is in progress. Sharma Lab continues to analyze O, H, and C isotopic composition of produced fluids collected from 3H and 5H.

Cole's Lab

Large-area analysis of mineralogy/rock fabric/organic matter (OM) associations in MSEEL sidewall core will continue. Analysis of fluid samples from the MIP 3H and 5H wells continues.

Wilkins Lab

New experiments are currently ongoing to investigate the attachment of cells onto fresh shale surfaces, which will be imaged using SEM.

Mouser's Lab

The team will continue working with the Wrighton Lab to mine the temporal metagenomics data for related lipid metabolism genes. The manuscript in preparation is expected to wrap up in early

fall. Andrea will be returning to MSEEL in mid-December to collect produced water from MIP 3H and 5H; geochemistry will be analyzed and all samples distributed to the MSEEL team at OSU.

Wrighton's Lab

Four manuscripts are in preparation from the Wrighton lab which incorporate MSEEL microbial community data.

Darrah's Lab

Ongoing analysis of isotopes will develop analyses to help improve bottom-up estimates of reservoir stimulation volumes by combining the produced fluid and solid noble gas data. The team will continue time-series analysis of fluid samples collected monthly from the MIP 3H and 5H wells. Additionally, several manuscripts (see above) are currently in the works.

Topic 4 – Environmental Monitoring – Surface Water & Sludge

Approach

The Marcellus Shale Energy and Environment Laboratory (MSEEL) is the first comprehensive field study coupling same site environmental baseline, completion and production monitoring with environmental outcomes. One year into the post-completion part of the program, the water and solid waste component of MSEEL has systematically sampled flowback and produced water volumes, hydraulic fracturing fluid, flowback, produced water, drilling muds, drill cuttings and characterized their inorganic, organic and radio chemistries. In addition, surface water in the nearby Monongahela River was monitored upstream and downstream of the MSEEL drill pad. Toxicity testing per EPA method 1311 (TCLP) was conducted on drill cuttings in both the vertical and horizontal (Marcellus) sections to evaluate their toxicity potential.

Previous findings

The MSEEL wells used green completion strategy including a synthetic based drilling fluid (Bio-Base 365). All drill cutting samples fell below TCLP thresholds for organic and inorganic components indicating that they are non-hazardous per the Resource Conservation and Recovery Act. Maximum specific isotopic activity in drill cuttings was recorded for 40 K which was 28.32 pCi/g. Gross alpha accounted for the highest reading at 60 pCi/g. The maximum combined radium isotope values was 10.85 pCi/g. These radioactivity levels are within the background range for the region.

The composition of the hydraulic fracturing (HF) fluids in both wells was similar to the makeup water which was drawn from the Monongahela River. Its chemistry was typical of Monongahela River water. This is true of inorganics, organics and radio chemicals. Organic surrogate recoveries were in the range of 90 to 104% indicating good quality control at the analytical laboratory. There was no evidence that Monongahela River quality was influenced by well development, completion or production at the MSEEL site.

Produced water is severely contaminated, indicating care in handling. Concentrations of all parameters increased through the flowback/produced water cycle. 226+228 Ra reached 20,000 pCi/L at post completion day 251 indicating an important trend that will be carefully assessed in ongoing monitoring.

Methods

Sampling schedule

Table 4.1 summarizes the produced water sampling schedule for the quarter. Produced water samples were taken at the upstream end of each well’s separator.

Table 4.1 Sampling schedule for the quarter.

	Freshwater		Aqueous/Solids: drilling/completion/production					total aqueous	total solids	Sampling Dates	Sampling Notes
	Mon River	Ground water	HF fluid makeup	HF fluids	flowback/produced	drilling fluids	drilling cuttings/muds				
Sampling Stations											
Flowback @ 580 weeks - 3H					1			1		7/12/2017	one sample 3H
Flowback @ 580 weeks - 5H					1			1		7/12/2017	5H offline
Flowback @ 2031weeks 4H					2			1		7/12/2017	4H offline
Flowback @ 2031 weeks 6H					1			1		7/12/2017	6H offline

Analytical parameters

Analytical parameters are listed in tables 4.2 and 4.3.

Table 4.2 Aqueous analytical parameters

Aqueous chemistry parameters - HF fluids and FPW***						
Inorganics				Organics	Radionuclides	
	Anions		Cations*			
pH	Br		Ag	Mg	Benzene	α
TDS	Cl		Al	Mn	Toluene	β
TSS	SO ₄		As	Na	Ethylbenzene	⁴⁰ K
Conductance	sulfides		Ba	Ni	Total xylene	²²⁶ Ra
Alkalinity	nitrate		Ca	Pb	m,p-xylene	²²⁸ Ra
Bicarbonate	nitrite		Cr	Se	o-xylene	
Carbonate			Fe	Sr	MBAS	
TP			K and Li	Zn	O&G	

Table 4.3 Analytical parameters drill cuttings and mud.

Solids chemistry parameters - Cuttings & Muds							
Inorganics			Organics	Radionuclides	TCLPs		
	Anions	Cations*					
alkalinity**	Br	Ag Mg	Propane	α	Arsenic	1,4-Dichlorobenzene	Methyl ethyl ketone
conductance	Cl	Al Mn	DRO	β	Barium	1,2-Dichloroethane	Nitrobenzene
pH	SO ₄	As Na	GRO	⁴⁰ K	Benzene	1,1-Dichloroethylene	Pentachlorophenol
bicarbonate**	sulfide	Ba Ni	Ethylbenzene	²²⁶ Ra	Cadmium	2,4-Dinitrotoluene	Pyridine
carbonate**	nitrate	Ca Pb	m,p-xylene	²²⁸ Ra	Carbon tetrachloride	Endrin	Selenium
TP	nitrite	Cr Se	o-xylene		Chlordane	Heptachlor	Silver
		Fe Sr	Styrene		Chlorobenzene	Heptachlor epoxide	Tetrachloroethene
		K Zn	Toluene		Chloroform	Hexachlorobenzene	Toxaphene
			Total xylenes		Chromium	Hexachlorobutadiene	Trichloroethylene
			TOC		o-Cresol	Hexachloroethane	2,4,5-Trichlorophenol
			COD		m-Cresol	Lead	2,4,6-Trichlorophenol
			O&G		p-Cresol	Lindane	2,4,5-TP (Silvex)
					Cresol	Mercury	Vinyl chloride
					2,4-D	Methoxychlor	

Results & Discussion

Produced water volume trends in wells MIP 3,5H and MIP 4,6H.

NNE’s water production logs were used to estimate produced water volumes. While water production rates were similar in the first two months post completion, cumulative water production rates soon diverged yielding very different curves for each well (Figure 4.1). It is noted that the older wells (4H, 6H) were shut in between 12 Dec 15 and 17 Oct 16, an interval of 315 days.

The proportion of hydrofrac fluid returned as produced water, even after 1844 days (5 years) was only 12% at MIP 4H and 7.5% at MIP 6H (Table 4.4). The reason for the variation among wells both respect to cumulative and proportional produced water returns remains an unanswered question.

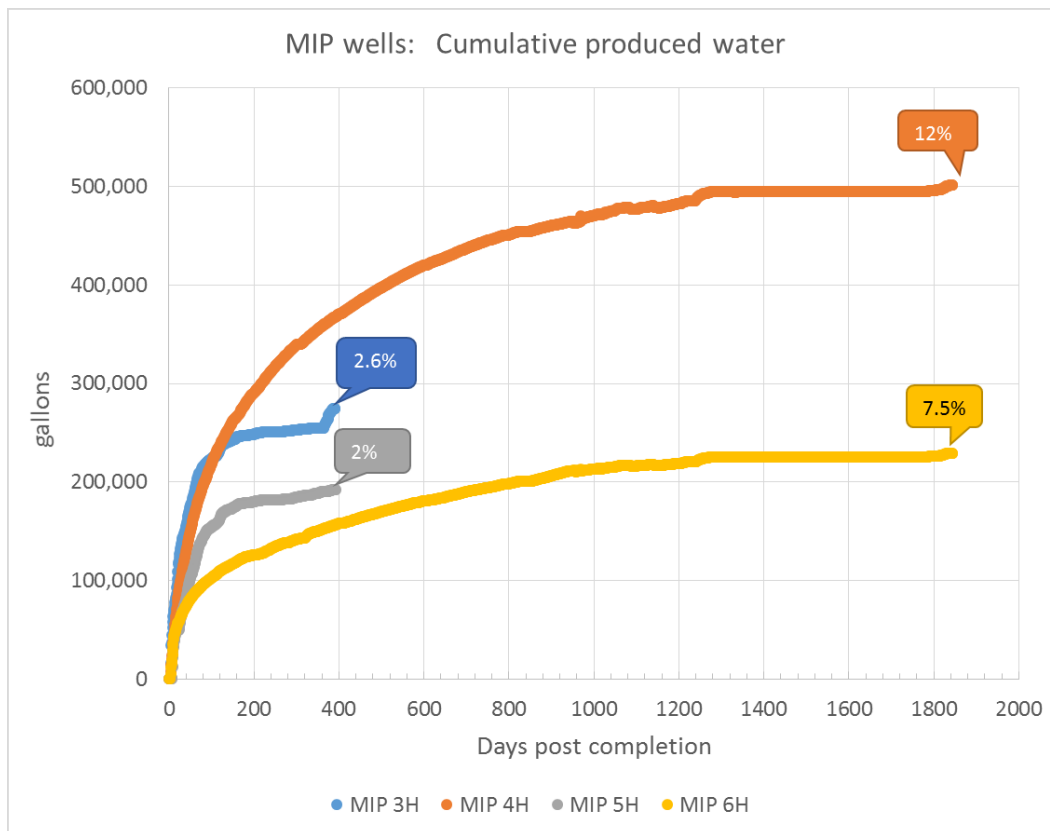


Figure 4.1. Cumulative water production at the four MSEEL wells.

Table 4.4. Produced water volumes relative to injected HF fluid for each MSEEL well.

	days post completion	cumulative produced water gal	% injected	HF injected gal
MIP 3H	392	274,102	2.6%	10,404,198
MIP 5H	392	192,134	2.0%	9,687,888
MIP 4H	1844	501,396	12.0%	4,160,982
MIP 6H	1844	229,183	7.5%	3,042,396

Trends in produced water chemistry

Major ions

While makeup water was characterized by low TDS (total dissolved solids) and a dominance of calcium and sulfate ions, produced water from initial flowback is essentially a sodium/calcium chloride water (Figure 4.2). Other than slight increases in the proportion of barium and strontium, the ionic composition of produced changed very little through 314 days post completion.

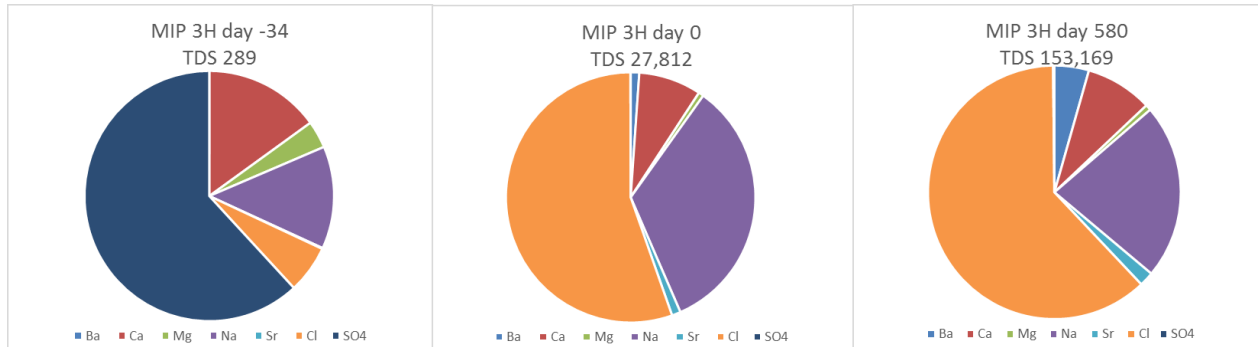


Figure 4.2 Changes in major ion concentrations in produced water from well MIP 3H. From left to right the charts represent makeup water from the Monongahela River, produced water on the first day of flowback and produced water on the 580th day post completion.

In fact, after 1935 days ionic composition remained nearly identical to the initial produced water (Figure 4.3).

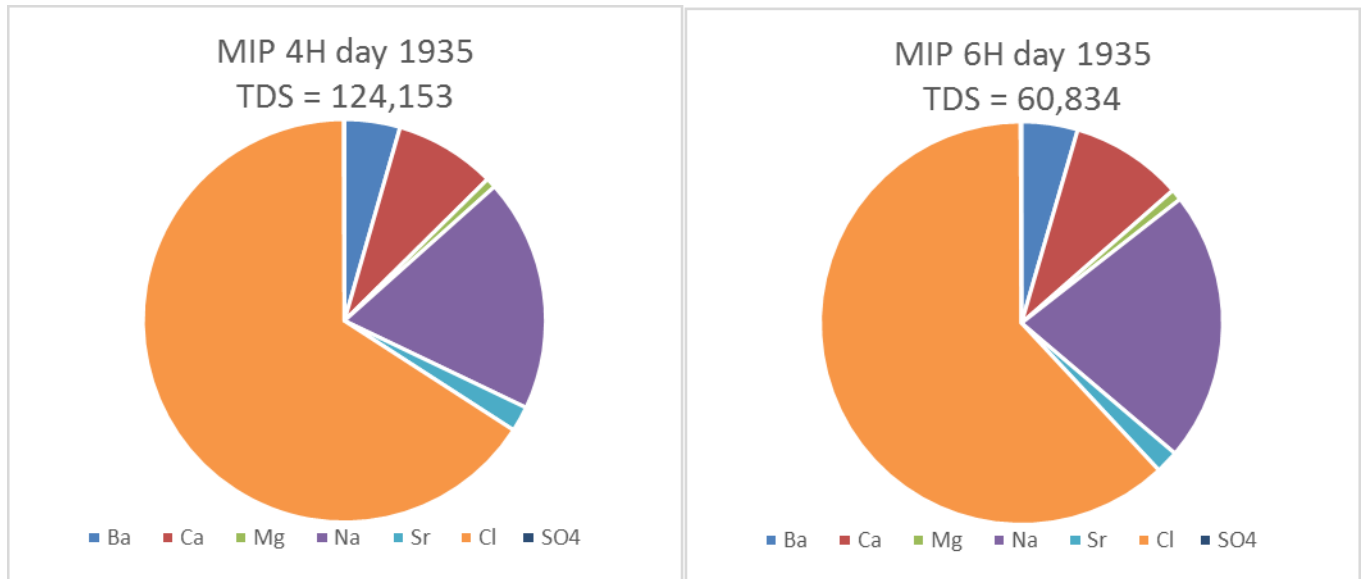


Figure 4.3 Major ion composition of wells MIP 4H and 6H 1935 days after completion.

While TDS increased rapidly over the initial 90 days post completion values had been consistently between 100,000 and 150,000 mg/L through day 580 and have since continued on an upward trend, increasing to around 180,000 mg/L for 3H (Figure 4.4). The older 4H and 6H

wells offer insight into the longer term TDS trend. Those wells only came back on line during this quarter after a shut in period of 315 days and those results vary but they are much lower than the current values for wells MIP 3H and 5H.

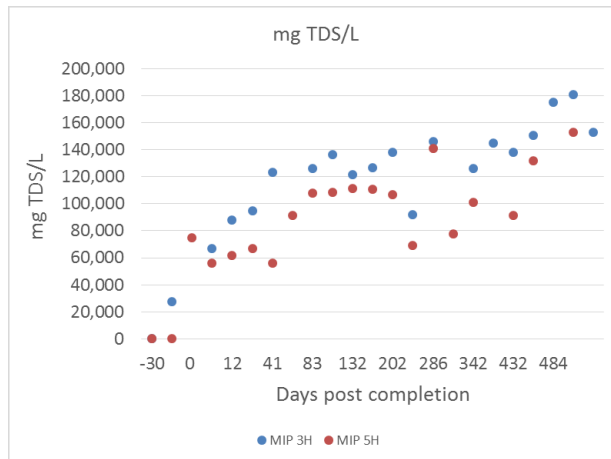


Figure 4.4 Changes in produced water TDS sdc (sum of dissolved constituents) through the first 580 days post completion (3,5H).

Water soluble organics

The water soluble aromatic compounds in produced water: benzene, toluene, ethylbenzene and xylene were never high. With one exception at post completion day 321, benzene has remained below 30 µg/L (Figure 4.5). This seems to be a characteristic of dry gas geologic units. After five years, benzene has declined below the drinking water standard of 5 µg/L.

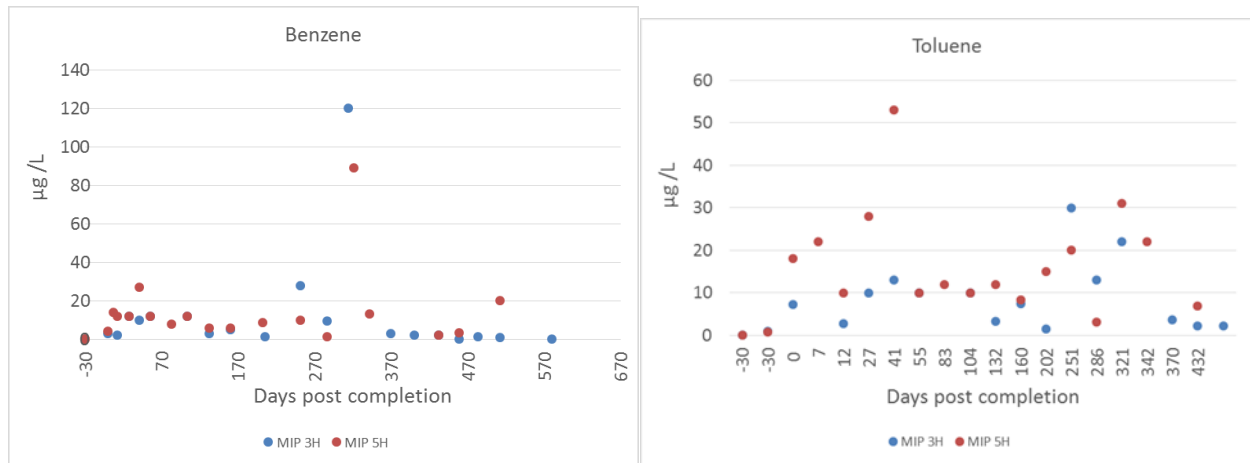


Figure 4.5 Changes in benzene and toluene concentrations. The figure shows data from well both 3H and 5H.

Radium isotopes

Radioactivity in produced water

Radium concentrations generally increased over the 580 days post completion at wells MIP 3H and 5H. Maximum levels of the radium isotopes reached about 20,000 pCi/L at the unchoked 3H well and about half that amount at 5H (Figure 4.6).

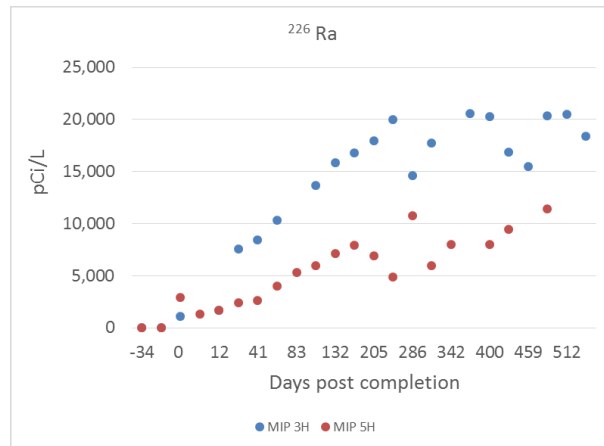


Figure 4.6 The radium isotopes are plotted against days post well completion. Well 5H was choked periodically. It produced less water and lower concentrations of radium.

At the older wells MIP 4H and 6H, all isotope concentrations declined to low levels, often below the MDC (minimum detectable concentration) (Table 4.5). This, like the apparent decline in TDS at the older wells is an interesting result and, if sustained by future sampling, would suggest exhaustion of contaminant reserves within the fracture field.

Table 4.5 Radiochemistry of the older wells 4H and 6H at 1828 (5 years) days post completion.

		16-Nov-16 MIP 4H			16-Nov-16 MIP 6H		
		days post completion: 1828			days post completion: 1828		
		act ¹	unc ²	mdc ³	act ¹	unc ²	mdc ³
α	pCi/L	228.0	53.6	27.2	57.7	10.9	1.6
β	pCi/L	48.7	20.1	29.2	7.4	1.6	0.8
²²⁶ Ra	pCi/L	353.3	260.6	309.2	199.3	333.5	390.3
²²⁸ Ra	pCi/L	31.1	31.9	48.6	0.0	20.9	54.6
⁴⁰ K	pCi/L	49.7	95.5	102.7	0.0	21.9	151.4

¹ activity

² +/- uncertainty

³ minimum detectable concentration

The radiochemical concentrations were determined by Pace Analytical in Greensburg PA, a state certified analytical lab. Figure 4.7 shows the relationship between gross alpha and ²²⁶Ra. The relationship between alpha and ²²⁶Ra is clear but the correlation coefficients show much more variance in the alpha readings. So, individual values can diverge to a far greater extent than the modelled values. Earlier studies (e.g. Ziemkiewicz and He, 2015) often relied on samples taken from several wells over short time spans so the apparent differences between alpha and,

individual isotope concentrations may well be analytical artifact. The MDCs and uncertainty levels reported by the lab indicated that both the alpha and radium levels were within ranges that would be considered reliable. This may illustrate the limitations of survey level parameters such as gross alpha.

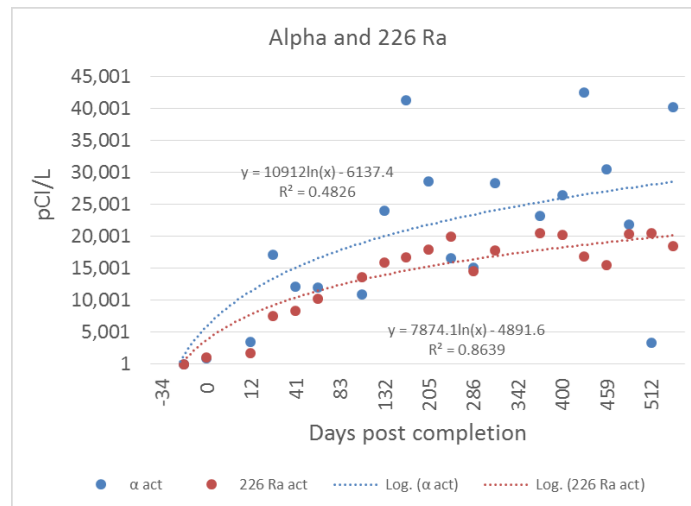


Figure 4.7. The relationship between gross alpha and ²²⁶Ra as a function of time post completion.

Solid waste

The TCLP (toxicity characteristics leaching procedure) or USEPA method 1311 is prescribed under the Resources Conservation and Recovery Act (RCRA) to identify hazardous solid waste. TCLP was applied to thirteen drill cutting samples, twelve from MIP 3H and 5H and one from another well in western Monongalia County. All three wells had been developed using green, synthetic drilling fluid. All samples fell below the TCLP criteria for hazardous waste and would be classified under RCRA subtitle D. Bio-Base 365 drilling fluid (Shrieve Chemical Products, Inc.) had been used at the MSEEL wells and ABS 40 (AES Drilling Fluids Inc.) was used at the other well.

Products

26 Jul 2017: URTeC, Austin, TX, Manuscript attached

27 Sep 2017: Marcellus Shale Coalition, Shale Insight, Press release attached

Plan for Next Quarter

The team will continue to sample and analyze flowback/produced water (FPW) from MIP 3H on a quarterly basis and other wells at 4H, 5H and 6H if they go back online. They will also collect for subtask 2.2.1b “produced water precipitate and perform toxicity and radiochemistry analyses” and begin development of chemical hygiene plan and set up for experiments of subtask 2.2.1c “chemical and biological factors influencing precipitate formation.”

References

Ziemkiewicz, P.F. and He, Y.T. 2015. Evolution of water chemistry during Marcellus shale gas development: A case study in West Virginia. *Chemosphere* 134:224-231.

Topic 5 – Environmental Monitoring: Air & Vehicular

Approach

The third Marcellus Shale Energy and Environment Laboratory (MSEEL) site assessment through West Virginia University (WVU) was carried out on July 19, 2017. The goal of this assessment was to measure the emissions of methane (CH₄) emitted, leaking or vented, from all onsite equipment. These measurements included an assessment of the enclosed gas production units (EGPUs), water tank, dehydration units, wellheads and stack emissions from the EGPUs were conducted to estimate the carbon dioxide (CO₂), carbon monoxide (CO), and oxides of nitrogen (NO_x) emissions, and CH₄ emissions from these sources. This was the first summer audit and showed interesting results. Since throughout was low and only one well is producing – the methane emissions were lower than previous audits by an order of magnitude – 0.035 kg/hr. With three audits completed, we have now compared results over time. The overall average of three MSEEL methane audits shows an average emission rate of 1.6 kg/hr. This is just under the arithmetic mean reported by Rella et al. – 1.740 kg/hr. Following is granular data for the third audit and comparison.

Results & Discussion

Methane fluxes were measured from all four wellheads on site. Leak rates were measured from the natural gas burner used for power generation. Methane loss rates from the enclosures of the EGPUs were also measured and were considered separately from the leaks. Emissions from the water tank were measured from the open hatch at the top of the tank. Background CH₄ concentration on site was determined to be 2.47 parts per million (ppm). The average methane lost from each wellhead is presented in Table 5.1.

Table 5.1: Methane Loss Rate from Wellheads

Component	CH ₄ Concentration above Background	CH ₄ Loss Rate	CH ₄ Loss Rate
	ppm	g/hr	kg/yr
MIP 3H	0	0	0
MIP 5H	1.51	.3	2.67
MIP 4H	.05	.01	.09
MIP 6H	5.74	1.33	11.68
Total		1.65	14.44

It can be seen from Table 5.1 that the methane losses from MIP 6H are much larger than those from the other wells are. Comparing the methane loss rate to the production generated by the wells, can provide insight as to if a well is leaking or venting during operation.

Table 5.2: Methane Loss Rate and Daily Production

Component	CH ₄ Loss Rate	CH ₄ Production Rate
	g/hr	MCF
MIP 3H	0	3153.75
MIP 5H	.3	0
MIP 4H	.01	0
MIP 6H	1.33	0
Total	1.65	3153.75

It is shown from Table 5.2 that MIP 3H was the only well in operation on the day of the site visit. MIP 6H had the greatest loss rate and the well was not in use. The methane losses from inside of the EGPU housing and the water tank were evaluated separately from the leaks since these emissions are a product of system design and are represented as methane losses. The results from the vents of the Exterran EGPU and the water tank are shown in Table 5.3.

Table 5.3: Methane Losses from EGPUs and Water Retainment Tank

Component	CH ₄ Concentration above Background	CH ₄ Loss Rate	CH ₄ Loss Rate
	ppm	g/hr	kg/yr
Tank	81.69	17.25	151.15
EGPU #1	242.32	8.43	73.81
EGPU #2	N/A	N/A	N/A
Total		25.68	224.96

Table 5.3 shows an extremely high concentration of methane loss from the water tank and the EGPU #1. The hatch on the tank was open during the site evaluation. This hatch is meant to be kept shut to limit the amount of methane lost from the tank. The EGPU #1 was open. The EGPU #1 was the main source of emissions. There were only two leaks were identified during this audit, coming from the thermoelectric generator creating power for the site. The leak rates are shown in Table 5.4.

Table 5.4: Methane Losses from On-site Leaks

Component	CH ₄ Concentration above Background	CH ₄ Loss Rate	CH ₄ Loss Rate
	ppm	g/hr	kg/yr
Thermoelectric Generator at Filter	45.78	8.43	73.81
Top of Thermoelectric Generator Exhaust	.09	.02	.14
Total		8.45	73.95

The Exterran stack emissions were also analyzed and showed emissions of CO₂, CO, CH₄, NO_x, C₂H₆, CH₂O and C₂H₂. These emissions contribute to the total greenhouse gas (GHG) emissions of the site and can be considered in estimating a total GHG emission rate on a CO₂-equivalent basis. The stacks were evaluated for carbon dioxide (CO₂), carbon monoxide (CO), Methane (CH₄), oxides of nitrogen (NO_x), ethane (C₂H₆), formaldehyde (CH₂O) and acetylene (C₂H₂). Only one stack could be evaluated at the time of the audit because the other did not contain a viable sample port. The stack velocity was measured with a pitot tube and the average velocity was determined to be 341.89 ft/min giving a flow rate of 268.52 standard cubic feet per minute (SCFM). Stack emissions were estimated by multiplying the concentration measured from a bag sample by the estimated flow rate are shown in Table 5.5.

Table 5.5: Emissions from Exterran Stacks

Emission	Concentration	Loss Rate	Loss Rate
	ppm	kg/hr	kg/yr
CO ₂	36021.58	9.1261	79944.74
CO	35.33	0.0057	49.90
CH ₄	22.81	0.0039	34.52
NO _x	1.09	0.0002	1.96
C ₂ H ₆	0.00	0.0000	0.00
CH ₂ O	0.19	<0.0001	0.28
C ₂ H ₂	0.00	0.0000	0.00

The total CO₂-equivalent GHG emissions from methane and CO₂ are shown in Table 5.6 assuming both Exterran units operated continuously with similar emissions profiles and that all emissions were continuous throughout the year. A CO₂-equivalent of 25 was used for methane [4].

Table 5.6: CO₂-Equivalent Greenhouse Gas Emissions (Both EGPUs Running)

Emission	CO ₂ -Equivalent	
	kg/yr	%
CO ₂	159,889	95.33
CH ₄	7,833	4.67
Total	167,723	

Methane losses were measured from a variety of site components including: wellheads, water retainment tank, enclosed gas production unit housings, stacks, and leaking devices. The total estimated methane emissions are shown in Table 5.7.

Table 5.7: Total Methane Losses

Source	Loss Rate	Loss Rate	Percent of Total Emissions
	g/hr	kg/yr	%
Wellheads	1.65	14.44	4.61%
Water Tank	17.25	151.15	48.24%
EGPU	8.43	73.81	23.55%
Leaks	8.45	73.95	23.60%
Total	35.77	313.35	

Comparing the values of the previous audits taken on April, 10 2017 and November 22, 2016 can be valuable to determine emissions trends of the components in question. Table 5.8 compares the methane loss of the three audits performed.

Table 5.8: Comparison to Previous Audits

Component	CH ₄ Loss Rate (g/hr)		
	Nov-16	Apr-17	Jul-17
Wellheads	0.85	139.43	1.65
EGPU Housing	356.50	69.89	8.43
Water Tank	83.98	3731.40	17.25
Leaks	227.40	163.10	8.45
NG Burner	0.82	N/A	N/A
Total	669.55	4103.81	35.77

A recent study by Rella, *et al.* used mobile flux techniques to estimate the total site emissions from well pads in the Barnett Shale region of Texas. In total 193 sites were audited and 122 were found to have measurable emissions rates. Other sites may or may not have had emission rates due to the measurement technique. Of the sites that had measurable fluxes, the geometric mean was 0.63 ± 0.09 kg/hr with an arithmetic mean of 1.74 ± 0.35 kg/hr. During audit 1, the MSEEL site emissions were 0.67 kg/hr, which is nearly identical to the geometric mean of Rella, *et al.*, and only about 1/3rd of their arithmetic mean. However, during audit 2 the methane emissions rate was 4.1 kg/hr or about 2.4 times the arithmetic mean of Rella, *et al.* Audit 3 had the lowest site emission rate with .035 kg/hr, which is about 20 times less than their geometric mean and 50 times less than their arithmetic mean. Figure 5.1 breaks down the total loss rate from Table 5.8 and compares it to the geometric and arithmetic means from Rella, *et al.*

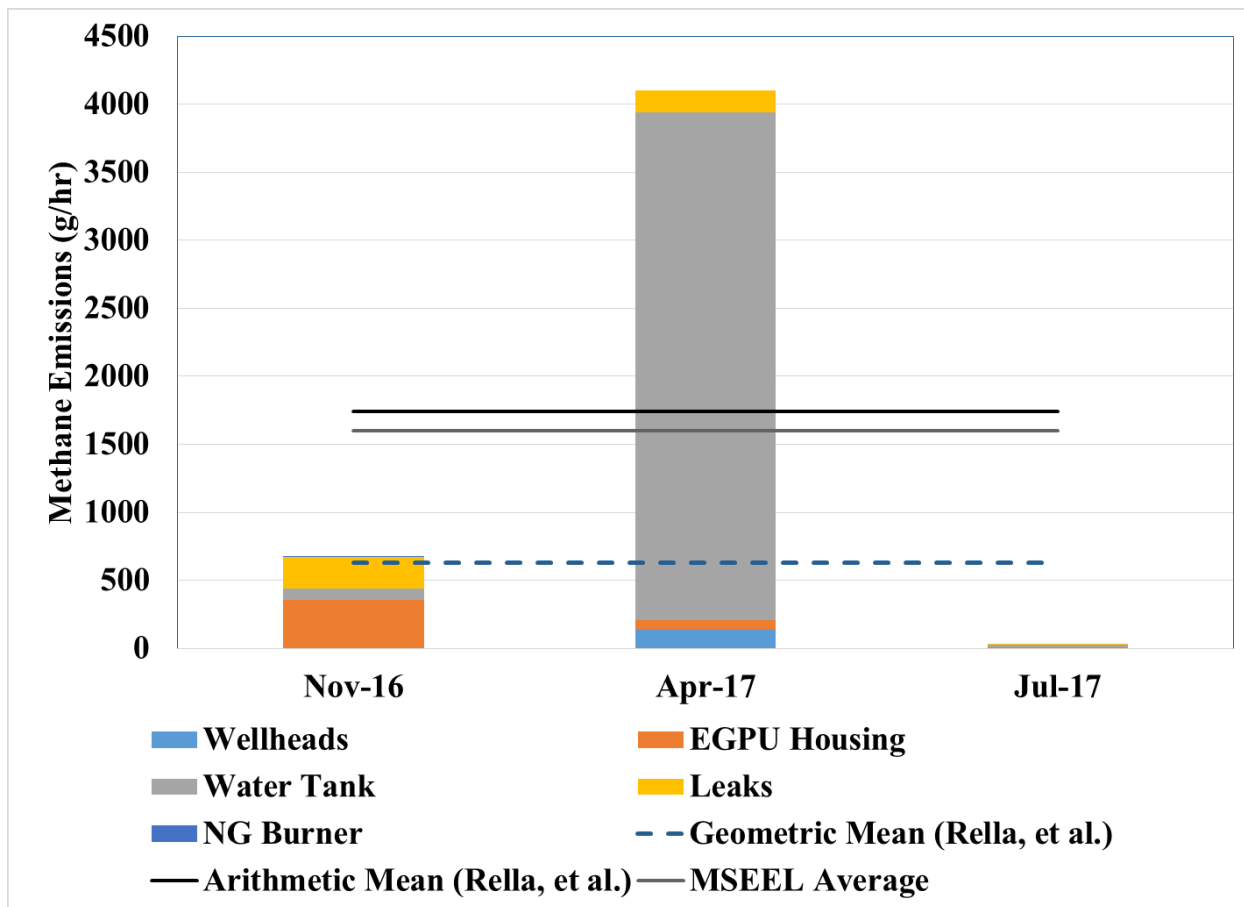


Figure 5.1: Breakdown of Leak Rate

Products

Data from the MSEEL audits have been used as seed data for an internal WVU grant under the O'Brien Seed funding opportunity. We have also updated a previous National Science Foundation proposal that will be submitted next quarter. The next quarter will also include a fourth audit. With this data, we may develop a conference paper or brief article summarizing the data to date. The data used from the drilling and fracturing engines was used as a part of a presentation Shale INSIGHT 2017. They have also been included in an abstract submitted to the AGU Fall meeting which was accepted for a poster presentation.

Plan for Next Quarter

- Complete the fourth site audit.
- Currently working with LI-COR to purchase a reduce price analyzer using the additional funds that were recently released.
- Begin preparation of a manuscript on MSEEL audits.

Topic 6 – Water Treatment

Approach

The team's first research activity of produced water treatment focuses on developing an (bio)electrochemical method to remove scale-forming cations as a pre-treatment system for produced water treatment. A two-chamber bioelectrochemical system used in this study contained an anode and cathode chambers separated by a cation exchange membrane. Each chamber contained graphite woven felt electrodes. An electric current was used to create a pH unbalance between the anode and cathode. The high-pH cathlyte was then used to treat raw produced water to remove multi-valent cations as a softening process. Produced water sample was collected at the MSEEL site and used in the study. The treatment method was shown to be effective in removing scale-forming cations.

Results & Discussion

Project had no activity this quarter.

Products

N/A

Plan for Next Quarter

N/A

Topic 7 – Database Development

Approach

Other than continued data uploading and quality control, including well production and pressure data, we have designed the structure for the public portal (Figure 7.1). This structure will be linked to the MSEEL.ORG site and provide seamless access to the raw data.

Results & Discussion

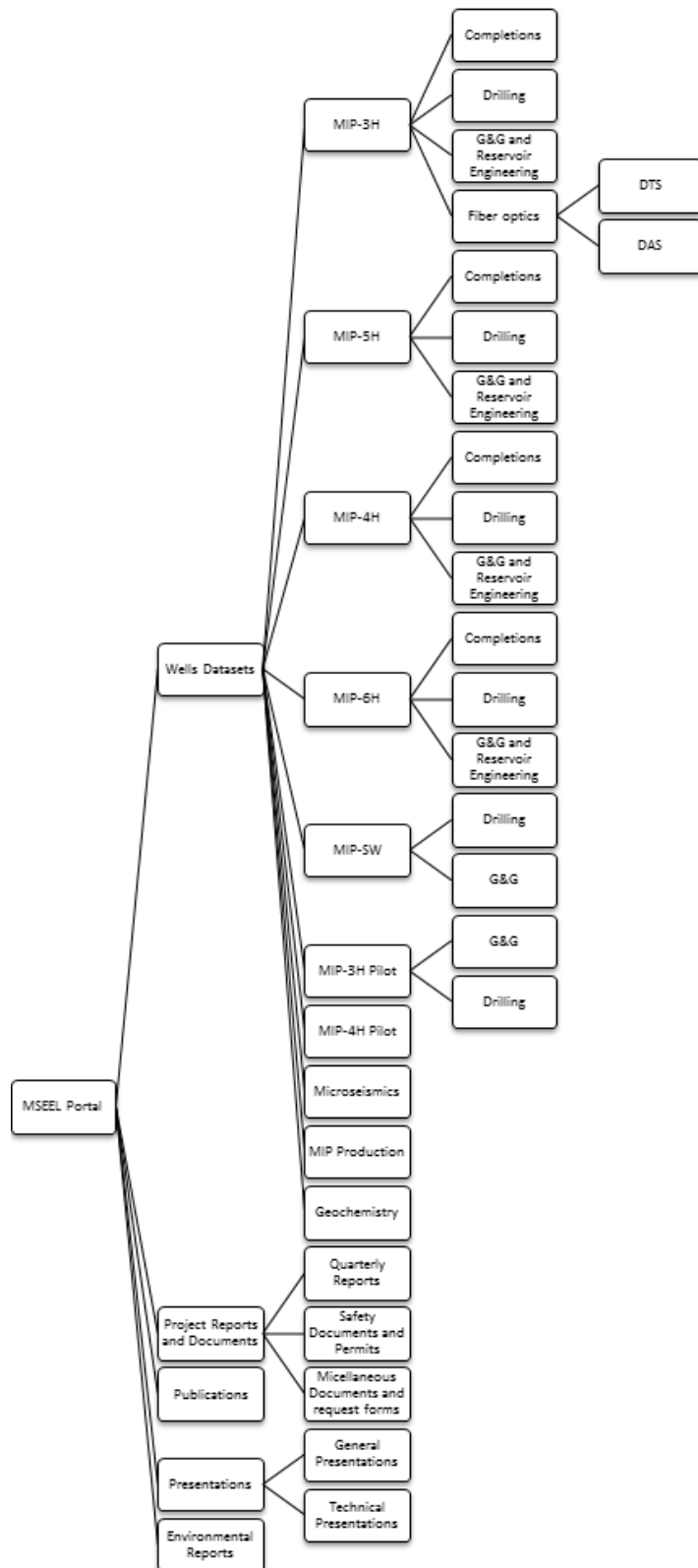


Figure 7.1 - Design structure for the public portal. This structure will be linked to the MSEEL.ORG site and provide seamless access to the raw data.

Products

N/A

Plan for Next Quarter

N/A

Topic 8 – Economic and Societal

This task is complete and will not be updated in future reports.

Cost Status

Year 1

Start: 10/01/2014 End:
09/30/2017

Baseline Reporting Quarter

	Q1 (12/31/14)	Q2 (3/30/15)	Q3 (6/30/15)	Q4 (9/30/15)
<u>Baseline Cost Plan</u>	(From 424A, Sec. D)			
<u>(from SF-424A)</u>				
Federal Share	\$549,000		\$3,549,000	
Non-Federal Share	\$0.00		\$0.00	
Total Planned (Federal and Non-Federal)	\$549,000		\$3,549,000	
Cumulative Baseline Costs				
<u>Actual Incurred Costs</u>				
Federal Share	\$0.00	\$14,760.39	\$237,451.36	\$300,925.66
Non-Federal Share	\$0.00	\$0.00	\$0.00	\$0.00
Total Incurred Costs - Quarterly (Federal and Non-Federal)	\$0.00	\$14,760.39	\$237,451.36	\$300,925.66
Cumulative Incurred Costs	\$0.00	\$14,760.39	\$252,211.75	\$553,137.41
<u>Uncosted</u>				
Federal Share	\$549,000	\$534,239.61	\$3,296,788.25	\$2,995,862.59
Non-Federal Share	\$0.00	\$0.00	\$2,814,930.00	\$2,814,930.00
Total Uncosted - Quarterly (Federal and Non-Federal)	\$549,000	\$534,239.61	\$6,111,718.25	\$5,810,792.59

Start: 10/01/2014 End:
09/30/2017

Baseline Reporting Quarter

	Q5 (12/31/15)	Q6 (3/30/16)	Q7 (6/30/16)	Q8 (9/30/16)
<u>Baseline Cost Plan</u>	(From 424A, Sec. D)			
<u>(from SF-424A)</u>				
Federal Share	\$6,247,367		\$7,297,926	
Non-Federal Share	2,814,930		\$4,342,480	
Total Planned (Federal and Non-Federal)	\$9,062,297	\$9,062,297.00	\$11,640,406	
Cumulative Baseline Costs				
<u>Actual Incurred Costs</u>				
Federal Share	\$577,065.91	\$4,480,939.42	\$845,967.23	\$556,511.68
Non-Federal Share	\$0.00	\$2,189,863.30	\$2,154,120.23	\$0.00
Total Incurred Costs - Quarterly (Federal and Non-Federal)	\$577,065.91	\$6,670,802.72	\$3,000,087.46	\$556,551.68
Cumulative Incurred Costs	\$1,130,203.32	\$7,801,006.04	\$10,637,732.23	\$11,194,243.91
<u>Uncosted</u>				
Federal Share	\$5,117,163.68	\$636,224.26	\$1,004,177.30	\$447,665.62
Non-Federal Share	\$2,814,930.00	\$625,066.70	(\$1,503.53)	(\$1,503.53)
Total Uncosted - Quarterly (Federal and Non-Federal)	\$2,418,796.68	\$1,261,290.96	\$1,002,673.77	\$446,162.09

Start: 10/01/2014 End:
09/30/2017

Baseline Reporting
Quarter

	Q9 (12/31/16)	Q10 (3/30/17)	Q11 (6/30/17)	Q12 (9/30/17)
<u>Baseline Cost Plan</u>	(From 424A, Sec. D)			
<u>(from SF-424A)</u>				
Federal Share				\$9,128,731
Non-Federal Share				\$4,520,922
Total Planned (Federal and Non-Federal)				\$13,649,653
Cumulative Baseline Costs				
<u>Actual Incurred Costs</u>				
Federal Share	\$113,223.71	\$196,266.36	\$120,801.19	\$1,147,988.73
Non-Federal Share	\$0.00	\$0.00	\$0.00	\$0.00
Total Incurred Costs - Quarterly (Federal and Non-Federal)	\$113,223.71	\$196,266.36	\$120,801.19	\$1,147,988.73
Cumulative Incurred Costs	\$11,307,467.62	\$11,503,733.98	\$11,624,535.17	\$12,772,523.90
<u>Uncosted</u>				
Federal Share	\$334,441.91	\$138,175.55	\$17,374.36	\$700,190.63
Non-Federal Share	(\$1,503.53)	(\$1,503.53)	(\$1,503.53)	\$176,938.47
Total Uncosted - Quarterly (Federal and Non-Federal)	\$332,938.38	\$136,672.02	\$15,870.83	\$877,129.10

National Energy Technology Laboratory

626 Cochran Mill Road
P.O. Box 10940
Pittsburgh, PA 15236-0940

3610 Collins Ferry Road
P.O. Box 880
Morgantown, WV 26507-0880

13131 Dairy Ashford, Suite 225
Sugarland, TX 77478

1450 Queen Avenue SW
Albany, OR 97321-2198

2175 University Ave. South
Suite 201
Fairbanks, AK 99709

Visit the NETL website at:
www.netl.doe.gov

Customer Service:
1-800-553-7681

